PIGMENT CELL & MELANOMA Research

An ongoing role for Wnt signaling in differentiating melanocytes in vivo.

Journal:	*Pigment Cell & Melanoma Research*
Manuscript ID	16-O-054.R2
Manuscript Type:	Original Article
Date Submitted by the Author:	25-Nov-2016
Complete List of Authors:	Vibert, Laura; University of Bath, Biology and Biochemistry Aquino, Gerardo; University of Surrey Faculty of Health and Medical Sciences, Department of Microbial and Cellular Sciences Gehring, Ines; University of California, Irvine, 3Developmental and Cell Biology School of Biological Sciences Subkankulova , Tatiana; University of Bath, Biology and Biochemistry Schilling, Thomas; University of California, Irvine, 3Developmental and Cell Biology School of Biological Sciences Rocco, Andrea; University of Surrey Faculty of Health and Medical Sciences, Department of Microbial and Cellular Sciences Kelsh, Robert; University of Bath, Biology and Biochemistry
Keywords:	differentiation, Specification, zebrafish, MITF, Wnt

An ongoing role for *Wnt* signaling in differentiating melanocytes *in vivo.*

Laura Vibert[1], Gerardo Aquino[2], Ines Gehring[3], Tatiana Subkhankulova[1], Thomas F. Schilling[3], Andrea Rocco[2] and Robert N. Kelsh[1]

Correspondence: Robert Kelsh email: bssrnk@bath.ac.uk

[1]*Developmental Biology Programme, Department of Biology and Biochemistry and Centre for Regenerative Medicine, Claverton Down, University of Bath, Bath, BA2 7AY, UK*
[2]*Department of Microbial and Cellular Sciences, Faculty of Health and Medical Sciences, University of Surrey, Guildford, GU2 7XH, UK*
[3]*Developmental and Cell Biology School of Biological Sciences, University of California, Irvine, 4109, Natural Sciences II, Irvine, CA 92697-2300, USA*

Total word count: 8878

Key words: *Wnt* signaling/ melanocyte/ specification/ differentiation/ zebrafish/ neural crest/ *mitfa*

Running title: Wnt signaling in differentiating melanocytes

Summary

A role for Wnt signaling in melanocyte specification from neural crest is conserved across vertebrates, but possible ongoing roles in melanocyte differentiation have received little attention. Using a systems biology approach to investigate the gene regulatory network underlying stable melanocyte differentiation in zebrafish highlighted a requirement for a positive feedback loop involving the melanocyte master regulator Mitfa. Here we test the hypothesis that Wnt signaling contributes to that positive feedback. We show firstly that Wnt signaling remains active in differentiating melanocytes and secondly that enhanced Wnt signaling drives elevated transcription of *mitfa*. We show that chemical activation of the Wnt signaling pathway at early stages of melanocyte development enhances melanocyte specification as expected, but importantly that at later (differentiation) stages it results in altered melanocyte morphology, although melanisation is not obviously affected. Downregulation of Wnt signaling also results in altered melanocyte morphology and organisation. We conclude that Wnt signaling plays a role in regulating ongoing aspects of melanocyte differentiation in zebrafish.

Significance

Gene regulatory networks underlie all aspects of the development of specific cell-types. While fate specification mechanisms and key genes associated with differentiation are often well-studied, mechanisms leading to maintenance of the differentiated state are less well understood, yet they are crucial from a disease perspective. Positive feedback loops are predicted to be crucial to these maintenance mechanisms. We predicted that such a feedback loop acting on *mitfa* would be crucial for melanocyte maintenance, and provided evidence supporting this hypothesis. Here we provide evidence for the first time that in zebrafish ongoing Wnt signaling is likely to contribute to this feedback loop.

Introduction

Melanocytes are a key derivative of the neural crest, and the mechanisms of melanocyte development are of major interest from developmental and stem cell biology and applied biology perspectives, with clear relevance to understanding human pigmentary disease (Yamaguchi and Hearing 2014; White et al., 2011; Speeckaert et al., 2014; Aoude et al., 2015; Mort et al., 2015). Melanocyte specification from neural crest cells has been relatively well-studied, and has illuminated the underlying mechanisms of neurocristopathies like the Waardenburg syndromes (Dutton et al., 2001; Lee et al., 2000; Southard-Smith et al., 1998; Elworthy et al., 2003). Numerous genes contributing to the differentiated melanocyte phenotype have been described, but little is known of how *stable*

melanocyte differentiation is maintained, although this is likely to be significant in understanding melanoma where reversion to a more progenitor-like state helps drive proliferation and invasiveness (White et al., 2011; Kaufmann et al., 2016). Stability of differentiation is likely to be an emergent property of the state of the gene regulatory network (GRN) in differentiated melanocytes.

Studies in both mouse and zebrafish have shown that melanocyte specification depends upon the expression in neural crest cells of *Microphthalmia-related Transcription Factor (Mitf; mitfa* in zebrafish), which encodes a basic Helix-Loop-Helix transcription factor (Steingrimsson et al., 1994; Hodgkinson et al., 1993; Lister et al., 1999; Watanabe et al., 2002; Opdecamp et al., 1997). *Mitf/mitfa* functions as the master regulator of melanocyte development as it controls all aspects of melanocyte cell biology including melanocyte survival, proliferation, morphology and melanogenesis itself (Steingrimsson et al., 2004; Cheli et al., 2010; Levy et al., 2006; Lister et al., 1999). Transcriptional activation of *Mitf/mitfa* depends upon Sox10, a transcription factor of the Sry-related HMG domain type, shown to bind directly to the *Mitf/mitfa* promoter (Hou et al., 2006; Kelsh 2006; Herbarth et al., 1998; Southard-Smith et al., 1998; Dutton et al., 2001; Elworthy et al., 2003). In addition, Wnt signaling, acting via Lef-1 and β-catenin mediated regulation of *Mitf/mitfa* transcription, is also required for melanocyte specification (Dorsky et al., 1998; Jin et al., 2001; Dorsky et al., 2000; Takeda et al., 2000; Dunn et al., 2000; Lee et al., 2004; Hari et al., 2012). Thus, the combined actions of early Wnt signaling and Sox10 drive expression of Mitf/Mitfa, which acts as a central node in the melanocyte GRN, activating numerous genes associated with all aspects of melanocyte differentiation (Cheli et al., 2010). Importantly, work in zebrafish has shown that a majority of neural crest cells express *mitfa* transiently, but only a subset form melanocytes (Curran et al., 2010). Thus maintenance of *mitfa* expression in a subset of neural crest cells is an important, but under-appreciated, aspect of melanocyte development and, indeed, likely represents a crucial part of the molecular basis for melanocyte fate commitment; cells in which *mitfa* expression is not maintained adopt alternative neural crest fates.

As a first step in understanding how this GRN results in stable maintenance of melanocyte differentiation, we used a systems biology approach, taking advantage of the zebrafish model to allow rapid iterative cycles of mathematical modelling and biological testing of a core melanocyte GRN (Greenhill et al., 2011). Three cycles of this approach resulted in an expanded core network that incorporated a number of hypothetical components for which we also provided experimental support (Fig. 1A; Greenhill et al., 2011). One of these hypothetical components was a predicted Factor Y that enabled stabilisation of melanocyte differentiation by contributing to a positive feedback loop regulating *mitfa* expression (Greenhill et al., 2011). We showed that whilst initial expression of *mitfa* is driven by Sox10*, sox10* then was gradually lost from differentiating melanocytes, being undetectable by *in situ* hybridisation or whole-mount immunofluorescence by c. 50 hours post

fertilisation (hpf). Importantly, we showed that continuing *sox10* expression is not required for melanocyte differentiation and indeed, may even delay this process. In the Greenhill study we showed that Mitfa itself contributed to maintenance of *mitfa* expression, but left the identity of other possible components of the feedback loop unknown.

The canonical Wnt pathway functions via regulation of nuclear β-catenin levels; Wnt protein binding to its transmembrane receptor, Frizzled, displaces glycogen synthase kinase-3β (GSK3β) from the destruction complex, preventing degradation of β-catenin in the cytoplasm, and resulting in elevated β-catenin levels in the nucleus where it functions as a transcriptional activator in co-operation with a co-activator, Lef-1 (Kofahl and Wolf, 2010, Barker, 2008). Canonical Wnt signaling drives fate specification of melanocytes via Tcf/Lef binding to *mitfa* regulatory elements (Dorsky et al., 1998; Dorsky et al., 2000; Takeda et al., 2000; Jin et al., 2001; Hari et al., 2012; Dunn et al., 2000; Lee et al., 2004) although the relevant Frizzled receptor remains elusive (Nikaido et al., 2013). In melanocyte fate specification, Wnt signaling functions in conjunction with Sox10 to drive *mitfa* expression; in a *sox10* mutant, *mitfa* expression is not detectable and melanocytes do not form (Dutton et al., 2001), suggesting that Wnt signaling alone is insufficient to drive *mitfa* expression.

Here we explore two possible modes by which Wnt signaling may also contribute to melanocyte maintenance: 1) by ongoing action alongside Sox10, and 2) in an Mitfa-dependent manner as a component of Factor Y (Figure 1A). We use a transgenic reporter line to show that Wnt signaling is active in melanocytes throughout both specification and differentiation phases. We then use small molecule stimulation of Wnt signaling showing first that it activates *mitfa* expression and is rate-limiting for melanocyte fate specification. We then use this approach to show that stimulating Wnt signaling during melanocyte differentiation affects melanocyte morphology and arrangement according to the timing of treatment. These shape changes correlate with upregulation of *mitfa* expression levels in melanocytes. These *mitfa* expression changes are independent of Mitfa activity in the specification and early differentiation phases, but depend upon Mitfa activity during late differentiation. Conversely, using a transgenic repressor of Wnt signaling, we show that inhibition of Wnt signaling during melanocyte differentiation stages also results in melanocyte shape changes. This is consistent with our proposal that Wnt signaling contributes to an Mitfa-dependent positive feedback loop that maintains melanocyte differentiation, in a manner consistent with our mathematical model of the core melanocyte GRN.

Results

Firstly we asked whether Wnt signaling was active in melanocytes during differentiation. We examined embryos carrying the *Tg(top:GFP)* reporter in which expression of a destabilised GFP

(dGFP) is driven by a promoter containing four consensus LEF1 responsive elements (Dorsky et al., 2002; van de Wetering et al., 1997; Korinek et al., 1997; Dorsky et al., 1998). We scored a sample of melanocytes from these fish throughout melanocyte differentiation (30-72 hpf), using a combination of immunofluorescent detection of dGFP and a low dose of PTU to partially inhibit melanisation to increase sensitivity. We readily detected the activation of dGFP in the tectum as previously described (Figure 1I; Dorsky et al., 2002). We also observed, for the first time, dGFP expression in melanocytes throughout the time-period examined (Figure 1B-G). At early stages the majority of melanocytes (78.5 %) had readily detectable dGFP expression, indicating that most cells at this stage were responding to a Wnt signal. At later stages, a significant proportion of cells still showed detectable dGFP expression, although by 72 hpf the proportion of cells was substantially lower (9 %), but this is likely to at least partly reflect the difficulties of detection of weak fluorescence in even partially-melanised cells.

Having shown that Wnt signaling remains active in melanocytes throughout their differentiation, we then tested the hypothesis that this Wnt signaling in melanocytes might contribute to regulation of their differentiation. We utilised a well-characterised GSK3β inhibitor, Bromoindirubin-3'-oxime (subsequently referred to as BIO), that has been used to investigate the effects of increased Wnt signaling in many model systems, including mammalian cardiomyocyte cell culture, melanoma cells (B16-F0), normal human melanocyte (NHM) cells, mouse embryonic stem cells, and zebrafish (Moro et al., 2012; Alexander et al., 2014; Bellei et al., 2010; Sineva and Pospelov, 2010; Kim et al., 2010; Bellei et al., 2008; Tseng et al., 2006). Consistent with its activation of Wnt signaling in our treated embryos, BIO treatment throughout a 15-40 hpf time-window activated dGFP reporter expression in *Tg(top:GFP)* fish, both in the tectum and in the melanocytes (Figure 1K-L); importantly, this BIO-treatment did not result in gross alterations to embryonic morphology.

Wnt signaling has been shown to drive melanocyte specification from the neural crest in both mouse and zebrafish (Dorsky et al., 1998; Hari et al., 2012). As a further positive control for the efficacy of BIO-treatment in modifying Wnt signaling in our fish, we tested the prediction that BIO treatment in the correct time window would increase melanocyte specification, resulting in elevated melanocyte numbers. We used a shorter treatment phase, focused on 15-30 hpf (Figure 2A), the time when melanocyte specification is thought to occur in the head and trunk. As expected, this treatment resulted in significantly increased melanocyte number in the head of treated embryos compared with controls (Figure 2B-E). Taking advantage of the developmental gradient in these embryos, we examined the trunk and tail region of embryos fixed at the same stage to examine whether elevated melanocyte numbers might be preceded by elevated *mitfa* expression in melanocyte progenitors (premigratory neural crest cells). Consistent with our current working model of the melanocyte GRN, BIO-treated embryos showed increased *mitfa* expression in premigratory neural crest cells compared

with mock-treated controls (Figure 2G-J). Our data suggest that the increased *mitfa* reflects increases in both the levels of *mitfa* expression within a cell and the number of *mitfa*-expressing cells (Figure 2D,E; compare with B,C), consistent with the predicted increase in melanocyte fate specification. Taken together our data support the conclusion that BIO treatment in a 15-30 hpf time-window results in elevated melanocyte specification through increased *mitfa* expression after activation of Wnt signaling. In addition, BIO-treated embryos show a reduction in ventrally-positioned *mitfa*+ cells, suggesting a transient inhibition of melanoblast migration.

Having validated BIO-treatment as an effective method for elevating Wnt signaling, we then addressed our hypothesis that ongoing Wnt signaling might be important for melanocyte differentiation and maintenance. In this study, we divided melanocyte differentiation into early and late phases according to *sox10* expression (Figure 3A). In the early differentiation phase (24-48 hpf) *sox10* expression in melanocytes is decreasing but still detectable by WISH and immunofluorescence, whereas in the late differentiation phase (48-72 hpf), *sox10* is not detectable by WISH or immunofluorescence (Greenhill et al., 2011). We analysed the consequences of boosting Wnt signaling via BIO treatment throughout the entire differentiation phase (24-72 hpf) and during each of the early and late phases of differentiation. Firstly, we tested whether these treatments gave any effects in terms of melanocyte cell number, focusing on the head region. In contrast to 15-30 hpf treatment, no increase in melanocyte number was observed after BIO treatment from 24-48 hpf (control, mean± s.d = 23.9±2.01; BIO, mean±s.d = 23.1±4.03, p=0.443), suggesting that Wnt-dependent melanocyte fate specification is complete in the head region by 24 hpf.

Next we assessed melanocyte differentiation, looking for any changes associated with BIO-treatment during the differentiation phases. In these BIO-treatments, we saw distinctive morphological changes to melanocytes, but interestingly the phenotype differed depending upon the period of BIO treatment. Embryos treated during the early differentiation time window and examined at 48 hpf displayed a dramatic increase in cell dendricity (Figure 3C,E) compared with mock-treated controls (Figure 3B,D). To quantitate this striking phenotype, we used Image J software to estimate the roundness parameter, an established formula relating cell perimeter and cell area (Figure 3F). We found BIO-treatment resulted in a significant increase in cell dendricity compared with mock-treated controls (mean±s.d: control, 2.44± 0.43; BIO, 4.25± 1.68, p = 0.004 (unpaired, one-tailed t-test)). Importantly, this change in cell shape at 72 hpf was not observed in 24-72 hpf (Figure 3G-N) or 48-72 hpf treatments (data not shown) suggesting that this aspect of cell differentiation was only sensitive to Wnt signaling for a period between 24 and 48 hpf, and that the shape changes were only transient. Indeed, where embryos treated in this way were examined at both 48 hpf and 72 hpf, we saw a clear dendricity phenotype at 48 hpf, but this had recovered by 72 hpf (data not shown). In contrast,

embryos treated with BIO from 24-72 hpf showed disorganised melanocytes in the dorsal head; cells were more dispersed, disrupting the 'U' or 'O'-shaped organisation typical of control embryos (Figure 3G-J). Treatment during the late differentiation phase alone (i.e. from 48-72 hpf) resulted in a similar phenotype (data not shown). A Multi-Distance Spatial Cluster Analysis using Ripley's K-Function (Ripley, B.D., 1977) was performed using spatstat package in R (Baddeley & Turner 2005) to quantify the decrease in patterned organisation of melanocytes in the dorsal head using comparable pictures of DMSO and BIO treated fish (Supp. Fig.1). We found that the Ripley's K function confirms the non-random organisation of melanocytes in dorsal heads of DMSO treated embryos (scale of analysis of r=35 pixels). Indeed, at this scale of analysis, for eight of the ten embryos the observed K value was smaller than the expected K value if cells were randomly spread (Supp.Fig.1, A,B,C,E,G,H,J). The result of the Ripley's K analysis performed on BIO treated embryos showed that, at r=35, the observed K values were found within the lower confidence envelop (in the grey area) of the graph meaning that cells were randomly spread in 90% of the cases in nine out of ten embryos (Supp.Fig1K-T). Conversely, 80% of the DMSO population shows a non-random cell organisation and 10% of the BIO treated population shows a non-random cell organisation. A Z-test was then performed to compare the two populations for cellular spatial organisation using the results of this analysis (at r=35, comparing « random » or « not-random »); the two populations were significantly different for this parameter (p-value =0.00164, $p < 0.01$). We conclude that treating embryos with BIO in the early phase of differentiation led to changes in cell shape, whereas ongoing BIO-treatment resulted in changed melanocyte arrangement.

Our working model of the melanocyte GRN predicted that *mitfa* transcription would be increased in response to activation of Wnt signaling. Using quantitative RT-qPCR, we saw a BIO-dependent increase in *mitfa* transcript levels after each of the treatment windows (Figure 4A). *mitfa* expression was increased by around five fold in embryos treated from both 24-48 hpf and 48-72 hpf whereas a nine-fold increase was observed in embryos treated from 24-72 hpf. Combining these data with the melanocyte phenotype changes observed above, we suggest that elevated *mitfa* expression can have distinct effects depending upon whether cells are in a plastic progenitor state (fate specification phase) or are committed to the melanocyte fate (differentiation phase).

Our model (Figure 1A) proposes two modes for Wnt action, one in conjunction with Sox10 and thus unlikely to be significant beyond 48 hpf when *sox10* expression in melanocytes is lost (Greenhill et al., 2011), and one as Factor Y, where it would function as part of a positive-feedback loop with Mitfa, and thus would be dependent upon active Mitfa. To test whether the increase in *mitfa* expression observed in BIO-treated embryos was 1) specific for melanocytes and 2) Mitfa-dependent, we used whole mount in situ hybridisation and RT-qPCR to assess *mitfa* expression in BIO treated *mitfa*^{w2} mutants (Figure 4B-H). The *mitfa*^{w2} mutant is a functional null allele, but expression of *mitfa*

transcripts can be assessed by in situ hybridisation (Johnson et al., 2010). In all cases, *mitfa* expression was restricted to cells with the morphology and distribution consistent with them being neural crest or melanocyte lineage cells, consistent with a cell-autonomous response. Importantly, BIO-treatment of *mitfa*^{w2} mutants in a 15-30 hpf window (i.e. during cell specification, when *sox10* is relatively strongly expressed in the melanocyte lineage) resulted in increased *mitfa* expression (Figure 4H), most clearly seen as increased numbers of cells expressing relatively high levels of *mitfa*, at 30 hpf compared with mock-treated embryos (Figure 4B,C). A 24-48 hpf BIO-treatment, assessed at 48 hpf, showed an elevated level of *mitfa* expression in *mitfa*^{w2} mutants, at least in the dorsal tail (Figure 4D,E). In contrast, BIO-treatment in a 24-72 (data not shown) or 48-72 hpf window (Figure 4F,G), assessed at 72 hpf, did not show elevated *mitfa* transcription in these *mitfa*^{w2} mutants (Figure 4H), suggesting that the Wnt-mediated effect is Mitfa-dependent. Quantitation of *mitfa* expression levels using RT-qPCR confirmed the significant increase in *mitfa* expression after 15-30 hpf treatment even in *mitfa*^{w2} mutants, and the absence of a significant response after the 24-72 and 48-72 hpf time-windows. Our quantitative assay did not detect the change after a 24-48 hpf time-window: although consistently detectable by the semi-quantitative whole-mount in situ hybridisation technique, which has the advantage of assessing individual cells in different spatial domains, this signal is apparently masked by the general signal coming from the head and trunk. We conclude that Wnt inputs on *mitfa* expression act initially through the Sox10-dependent mechanism, but then switch to functioning through a Sox10-independent, Mitfa-dependent positive feedback loop.

As a complement to these gain-of-function studies, we tested the effects of loss of Wnt signaling activity during melanocyte differentiation using a conditional activation of the dominant negative T-cell Factor 3 (Tcf3) in transgenic zebrafish carrying *Tg(hsp70l:tcf3-deltaC-GFP)* (Martin and Kimelman, 2012). As before, we tested the functionality of our experimental system by inducing heat-shock during the specification phase of melanocyte development, from 15 to 28 hpf, and assessing first activation of GFP fluorescence and expression of Wnt signaling targets such as *mitfa*, by RT-qPCR. Both activation of GFP and downregulation of *mitfa* expression were observed after heat-shock (data not shown). To assess the requirement for ongoing Wnt signaling in melanocyte differentiation, we heat-shocked embryos at each of four timepoints, 29 hpf, 36 hpf, 48 hpf, and 62 hpf before assessing melanocyte phenotypes in the dorsal head at 73 hpf. Two populations of embryos could be distinguished by the level of activation of GFP, one where embryos showed strong GFP fluorescence and the second population showing weak GFP fluorescence; we note that in almost all cases melanocytes were abundant, indicating that survival of melanocytes was usually not affected, although in a subset of the fish exhibiting strong GFP, melanocyte number was visibly reduced. In the first population (strong inhibition of Wnt signaling) melanocyte melanisation, apparent morphology and patterning were all abnormal, but since the gross anatomy of the embryos was also affected, these melanocyte phenotypes were not quantitated. However, we noticed that a subset of melanocytes in

each fish was abnormally rounded, melanisation was always reduced and these cells were abnormally patterned (Supp. Fig. 2). In the second population (weak inhibition of Wnt signaling), melanocyte morphology was more normal, but their patterning was modified compared to non heat-schocked siblings (Figure 5). We observed enhanced clustering of melanocytes, particularly in the posterior region of the dorsal head (Figure 5B,D,F,H, blue arrow). Again, we used Multi-Distance Spatial Cluster Analysis using Ripley's K-Function (Ripley, B.D. (1977)) to quantify the change in patterned organisation of melanocytes in the dorsal head using comparable pictures (Supp. Fig. 3). This analysis showed that whereas 90% of the non-heat-shocked *Tg(hsp70l:tcf3-deltaC-GFP)* embryos showed "non-random" pattern, 70 % of the heat-shocked *Tg(hsp70l:tcf3-deltaC-GFP)* embryos showed loss of organisation (« random » cell organisation – the combination of the clustered melanocytes in the posterior head and the unclustered melanocytes in the anterior head are together scored by the algorithm as more randomly organised using this scale of analysis)(scale of analysis of r=50 pixels). A Z-test comparing the two populations for cellular spatial organisation using the results of this analysis (at r=50, comparing « random » or « not-random ») showed they were significantly different for this parameter (p-value = 0.00244, $p < 0.01$). We conclude that inactivating Wnt signaling during melanocyte differentiation in *Tg(hsp70l:tcf3-deltaC-GFP)* using heat shock led to significantly increased clustering of melanocytes in the posterior part of the dorsal head. We note that this loss-of-function phenotype is complementary to the gain-of-function phenotype using drug treatment, suggesting that Wnt signaling has a consistent impact on melanocyte differentiation in zebrafish *in vivo*.

We used the mathematical modelling approach we developed before (Greenhill et al., 2011) to assess the effects of including Wnt signaling (Supp. Fig. 3A). We incorporated Wnt signaling in both fate specification and differentiation phases by assuming Wnt expression to activate β-catenin/Lef-1 (abbreviated as T), coupled in turn with an AND gate to Sox10 during specification, and by another AND gate to Mitfa during commitment. For such a highly migratory cell-type, melanocyte fate specification (in/near the dorsal neural tube) and melanocyte differentiation (during dispersion and in post-migratory locations) are usually anatomically distinct and, given the complexity of Wnt expression patterns, thus are intuitively likely to involve distinct Wnt family members. Thus, we postulated two independent Wnt signals, one (WntA) acting in an early, but transient, time window lasting to approximately 30 hpf, and another (WntB) beginning at that latter time point and extending throughout differentiation. We also assumed a threshold level of T required to trigger a response from the AND gate between Sox10 and T (Supp. Fig.3A,B), and a threshold level of Mitfa to avoid accidental activation of the Mitfa feedback loop (see Greenhill et al., 2011). As in Greenhill et al. (2011) one of the key outcomes used to judge the appropriateness of the subsequent simulations was that *mitfa* expression initially rose, and then was maintained at a substantial level. Indeed, under normal conditions our revised model results in expression profiles comparable to those of the original

Greenhill Model C (Greenhill et al., 2011). Moreover, modelling the effects of mutating the two Wnt signals independently behave as expected intuitively (Supp. Fig. 3C,D). In particular, in the absence of the first Wnt signal, WntA, melanocyte specification fails and *mitfa* expression remains absent (Supp. Fig. 3C); likewise, in the absence of the second Wnt signal, WntB, *mitfa* expression peaks transiently before disappearing rapidly, so that maintenance of the differentiated state fails (Supp. Fig. 3D). Currently, Wnt8 has been proposed as an inducer of neural crest in zebrafish (Lewis et al., 2004), but knowledge of the Wnt signals underlying melanocyte development in fish is very limited, although Wnt8 has been shown not to be critical (Dorsky et al., 1998; Lewis et al., 2004); a testable prediction of our modelling is that two distinct Wnt signals drive early melanocyte fate specification versus later maintenance of differentiation.

We then assessed *in silico* the effect of increasing Wnt signaling strength in each of the specification and (early, late and full) differentiation phases. We did this by modifying the amount of WntA and WntB driving expression of T, and simulating accordingly the GRN response. We modelled the derepression of the Wnt signal due to the action of the BIO-treatment as a linear increase in time of WntA/B. As a consequence we expected the elevated expression of *mitfa* induced by BIO to be proportional to the duration of the BIO-treatment. Indeed, by choosing parameter values compatible with values in the literature (see Materials and Methods), the simulations show a relative increase of Mitfa expression in response to BIO compatible with the experimental data (Fig. I). In particular we show that when BIO is applied for the same amount of time (namely in the time windows 24-48hpf and 48-72hpf) the increase in *mitfa* is approximately the same. In contrast, when BIO is applied between 24-72 hpf, our simulations show a larger *mitfa* increase, roughly comparable with the observed linear dependency. Thus, our revised model with its more precise delineation of the roles of Wnt signals at different phases in melanocyte development continues to correspond well to the key experimental observations *in vivo*.

Our observation that elevated Wnt signaling in the specification phase results in more cells becoming melanocytes is readily accounted for by the model through the threshold on T. The likelihood of an *mitfa*-expressing cell maintaining *mitfa* expression and thus differentiating into a melanocyte depends on T being above this threshold in the specification phase. In a population of cells, we expect stochastic variations in the levels of WntA (and hence T) will result in this condition not being satisfied in some cells. If BIO is applied early, T levels are enhanced, and therefore during the specification phase (i.e. prior to commitment) the proportion of cells proceeding successfully towards the melanocyte state is predicted to increase. In contrast, if BIO is only applied later, T levels during the earlier specification window are unaffected, so no change in the final number of melanocytes is predicted, in agreement with our experimental data.

Discussion

We conclude that in addition to the established role for Wnt signaling in melanocyte specification from the neural crest, Wnt signaling has an ongoing influence on melanocyte differentiation at least until 72 hpf. By using a transgenic reporter strain we demonstrated that Wnt signaling remained detectable in differentiated melanocytes until 72 hpf at least. We then used BIO to assess the effects of increased Wnt signaling on melanocyte development in zebrafish embryos, showing that such treatment resulted in elevated *mitfa* expression in the neural crest and melanocyte lineage cells. Interestingly, we observed defects in melanocyte morphology with an increase in cell dendricity at 48 hour post fertilisation (hpf) and altered cell organisation at 72 hpf. We complemented these gain-of-function studies with a loss-of-function approach, using a conditional dominant negative transgenic line to inhibit Wnt signaling activity during melanocyte differentiation phases. Importantly, our data showed that this resulted changes in melanocyte morphology (when dnTcf3 strongly expressed), resulting for example in enhanced clustering of melanocytes in the posterior head. This study demonstrates for the first time a function for Wnt signaling in zebrafish melanocytes, beyond the well-known role in melanocyte fate specification, showing that it is important for multiple aspects of melanocyte differentiation. We note that our data indicates that the mode of Wnt signaling input changes from an Mitfa-independent/Sox10-dependent early role to an Mitfa-dependent/Sox10-independent later role, suggesting that Wnt signaling at late stages becomes incorporated into the melanocyte maintenance (Factor Y) role postulated in our earlier work. We have revised our working model of the core GRN of melanocyte development in zebrafish to incorporate these new data (Figure 4J). It is likely that Wnt signaling has a similar role in mammalian melanocytes since GSK3β inhibition results in upregulation of *MITF* expression and differentiation in normal human melanocytes, at least in cell culture (Bellei et al., 2008).

Although we show here that Wnt signaling continues to influence melanocyte differentiation, our gain-of-function experiments do not cause obvious effects on melanisation. However, we note that our modelling data (Supp. Fig. 3E,F) indicates that this may be quantitatively relatively subtle (e.g. for *dct* in curves shown), so our failure to detect such an effect in vivo may be simply due to lack of sensitivity in our assay. A study of normal human melanocytes in tissue culture showed that GSK3β inhibition stimulated melanogenesis through activation of *MITF* (Bellei et al., 2008). In contrast, in our loss-of-function experiments, those embryos showing highest levels of GFP and in which Wnt signaling was presumably most inhibited, showed a pronounced reduction in both melanin levels and defects in apparent cell morphology. Thus, it seems that Wnt signaling is important for all aspects of melanocyte differentiation, consistent with its effects on expression of *mitfa*.

The role for Wnt/β-catenin signaling in melanocyte specification through induction of *Mitf* expression is conserved in fish and mammals (Dorsky et al., 2000; Takeda et al., 2000). Our work showing that inhibition of GSK3-β using BIO stimulates melanoblast specification (*mitfa* expression) adds further support to this conclusion. Importantly, no increase in melanocyte cell number in the dorsal head was observed after 24-72 hpf treatments suggesting that melanocyte specification from neural crest cells does not extend much beyond 24 hpf. Furthermore, our time window studies showed that treatment from 15-30 hpf was sufficient to generate elevated numbers of head melanocytes that persist until at least 72 hpf, whereas treatment in a 24-48 hpf window did not. These data indicate, for the first time to our knowledge, that commitment to the melanocyte fate in zebrafish (at least for melanocytes in the head region that arise in the embryo) has occurred by c. 30 hpf. As explained above, melanocyte specification reflects *maintenance* of *mitfa* expression in NCCs, so our data suggest that this process is limited by Wnt signaling.

Our data demonstrate intriguing Wnt-dependent effects on melanocyte morphology and organisation. An *in vitro* study of normal human epidermal melanocytes demonstrated that increased and decreased levels of active β-catenin resulted in increased and decreased cell dendricity respectively *(*Kim et al., 2010). They further showed that this resulted from activation of distinct downstream modulators, PKCf and PKCd, respectively (Kim et al., 2010). They showed that overexpression of PKCf resulted in the decrease of protein levels for Rac1 and Cdc42 and consequently a reduction of dendrite formation in melanocytes, while overexpression of PKCd led to increase of Rac1 and Cdc42 and an increase in melanocyte dendrites. We show here that elevated Wnt signaling results in increased *mitfa* expression and increased dendricity, suggesting a causal link between *mitfa* expression levels and cell shape. This idea is strongly supported by earlier studies in Xenopus embryos showing that increased *X-mitfa* expression resulted in increased melanocyte dendricity and cell dispersal (Kumasaka et al., 2005; Kawasaki et al., 2008). Further studies will be required to test whether Wnt signaling in zebrafish causes increased melanocyte dendricity through a pathway of *mitfa*-dependent activation of PKCd, elevated levels of activated Rac and Cdc42, and consequent modifications of the actin cytoskeleton.

In summary, our work defines two phases of Wnt signaling involvement in zebrafish melanocyte development *in vivo*, both of which are likely conserved in mammals. Recent analysis showed that the two transcription factors Tfap2a and Tfap2e are required for early melanocyte differentiation, through both maintenance of *kit* expression and another mechanism still to be defined (Van Otterloo et al., 2010). It will be of interest to assess whether these roles for Tfap2 factors extends to ongoing maintenance of the differentiated state and, if so, the extent to which Wnt signaling and Tfap2/Kit function are integrated in this system.

Figure legends

Figure 1.

Ongoing Wnt signaling is detectable in differentiating melanocytes.

(A) Diagram of working model for melanocyte core GRN (modified from Greenhill et al., 2011). Note two inputs from Wnt signaling on *mitfa* expression, one well-established role acting alongside Sox10 driving melanocyte fate specification, and hypothetical role explored here as part of a positive feedback loop also involving Mitfa itself. B-G) Wnt signaling in differentiating melanocytes was assessed by scoring samples of melanocytes for detection of dGFP by immunofluorescence in *Tg*(*top:GFP*) transgenic embryos from 30-72 hpf. GFP-positive melanocytes (arrows) are shown by immunofluorescence (B,D,F) and DIC (C,E,G) to show melanin pigment. At each stage, 30 melanocytes in each of 15 embryos were assessed for GFP expression, in the dorsal head and throughout the dorsal and lateral trunk; numbers show the percentage of melanocytes expressing GFP (mean ± s.d) at corresponding stages (n = 450 per stage). H) Schematic showing timing of BIO treatment used. I-L) BIO-treatment enhances activity of *Tg(top:GFP)* reporter. BIO-treatment from 15 hpf to 40 hpf dramatically enhances dGFP expression (red arrows) in the tectum of treated (K) compared with mock-treated controls (I) and also increases dGFP signal in melanocytes of *Tg(top:GFP)* embryos (BIO-treated (L) compared with mock-treated control (J)). All images, lateral views using confocal microscopy. EM, embryo medium; e: eye; T: tectum. Scale bars: B-G) 10 µm; I-L) 100 µm.

Figure 2.

Elevated Wnt signaling in melanocyte specification time window increased numbers of melanocytes. A) Schematic showing timing of BIO treatment or control mock-treatment (DMSO alone) used. B-E) Lateral views of the trunk of live 30 hpf zebrafish embryos showing melanocytes (red arrows); note increased number in both anterior (D) and posterior trunk (E) of embryos treated with 5 µM BIO compared with control DMSO treated embryos (B,C respectively). F) Quantitation of increased melanocyte number in heads of BIO-treated embryos (mean ± s.d.; control, 13 ± 2.1; BIO, 32 ± 5.3, $p<10^{-6}$) (n= 20; *** indicates significant difference between treated and mock-treated; unpaired, one-tailed t-test). G-J). Lateral views of posterior trunk (G,I) and close-up of anterior tail (H,J) of 30 hpf zebrafish embryo in situ hybridisations to show *mitfa* expression in embryos treated with BIO (I,J) or DMSO control (G,H). In the DMSO control embryos (G,H) discontinuous *mitfa* expression is observed in the dorsal region (blue arrows show discontinuities of the signal), whereas in the BIO treated embryos (I,J) *mitfa* expression is continuous throughout the dorsal region (red arrows). Images show representative phenotypes (n=20 per treatment). Scale bar: 100 µm.

Figure 3: Elevated Wnt signaling in melanocyte differentiation time window alters melanocyte morphology. A) Schematic of melanocyte differentiation BIO-treatment time-windows. B-E)

Activation of Wnt signaling in early differentiation period (24-48 hpf) increases melanocyte dendricity and dispersion. Lateral view at 48 hpf of head of live embryos treated with control DMSO (B) or BIO (C) from 24-48 hpf. Panels D and E show enlargements of head melanocytes from embryos in B and C respectively. F) Quantitation of dendricity: the cell roundness parameter was calculated for each melanocyte as R = P2/4∏A, where A is the cell area and P the cell perimeter, 20 cells were investigated (n=20) in 10 different embryos for each condition. A score of R=1.0 represents a perfectly round melanocyte; increased R values represent increased dendricity. Control, R=2.44 ± 0.43, BIO R= 4.25 ± 1.68, p = 0.004, t-test result, p-value<0.01 (**). G-J) Elevated Wnt signaling throughout full differentiation or during late differentiation window only affects melanocyte organisation. Red line in G indicates the dorsal head melanophores which usually approximate an O- or U-shaped pattern, although often with extra branches as in this specific example. Dorsolateral view at 72 hpf of heads of live embryos treated with control DMSO (G,I,K,M) or BIO (H,J,L,N) from 24-72 hpf shown. Note that embryos treated in only Late Differentiation window (48-72 hpf) show equivalent phenotype (data not shown). Embryos shown are representative of samples examined (n=160 zebrafish embryos for each treatment). Scale bars: 100 µm (B,D,G,I).

Figure 4: Positive feedback between Wnt signaling and Mitfa during late differentiation phase of melanocyte development. A) Quantitation of *mitfa* expression by RT-qPCR showing significantly increased levels in BIO-treated embryos compared with untreated controls; data are expressed as percentage of mock-treated controls (control *mitfa* level = 100 % transcripts (red line on graph)). Gene expression was investigated in 10 samples consisting of the trunk and tail of 50 embryos for each condition and in triplicate, after normalisation to the stable expression of a reference house-keeping gene, *gapdh*. All treatments caused significant increase of *mitfa* expression (t-test, two- tailed: 24-48 hpf, 535±7.1 (p= 0.00087); 48-72 hpf, 496±9.8(p= 0.0085); 24-72 hpf, 872±32.1 (p = 0.000092). ***, p-value<0.001). B-G) Activating Wnt signaling after 48 hpf does not affect *mitfa* expression in *mitfa*^{w2} mutant embryos during melanocyte differentiation. Lateral views of trunk showing in situ hybridisation for *mitfa* expression in *mitfa* mutant fish. *mitfa* mutant embryos treated with BIO in the melanocyte specification phase (15-30 hpf) (C) showed increased *mitfa* expression (purple) compared to DMSO-treated embryos (B). Similarly, *mitfa* mutant embryos treated with BIO in the melanocyte early differentiation phase (24-48 hpf) (E) showed increased *mitfa* expression in tail dorsal stripe melanocytes compared to DMSO-treated embryos (D). In contrast, *mitfa* mutant embryos treated with BIO throughout the late melanocyte differentiation phase (48-72 hpf) (G) did not show increased *mitfa* expression compared to DMSO-treated embryos (F) at 72 hpf. 40 zebrafish embryos were investigated for each condition; BIO-treated and matched control embryos were processed for in situ hybridisation in parallel and under identical conditions. H) Quantitation of *mitfa* expression by RT-qPCR showing significantly increased levels in BIO-treated embryos at 30 hpf compared with untreated controls but not at 48 hpf nor at 72 hpf; data are expressed as percentage of mock-treated

controls (control *mitfa* level = 100 % transcripts (red line on graph)). Gene expression was investigated in triplicate, after normalisation to the stable expression of a reference house-keeping gene, *gapdh*. Only 15-30 hpf treatment caused significant increase of *mitfa* expression (t-test, two-tailed: 15-30 hpf, 160.39±7.27 (p=0.0020); 24-48 hpf, 108.15±7.9 (p= 0.0675); 24-72 hpf, 104.6±8.36 (p= 0.544); 24-72 hpf, 86.14±8.96 (p = 0.0831). **, p-value<0.01). I) The effect of the three BIO-treatments applied in the 24-48, 48-72 and 24-72 hpf time windows is shown on Mitfa only as compared to the case of no treatment. The 24-48 and 48-72 hpf BIO-treatments induce an approximately equal increase of Mitfa as measured at the end of the treatment. J) Revised GRN model. Scale bars: 100 μm

Figure 5: Inactivation of Wnt signalling during melanocyte differentiation enhances melanocyte clustering in posterior dorsal head. *Tg(hsp70l:tcf3-deltaC-GFP)* embryos were heat shocked at 29 hpf, 36 hpf, 48 hpf and 62 hpf and observed at 73 hpf (B, D, F, H) and compared to control non-heat-shocked transgenic *Tg(hsp70l:tcf3-deltaC-GFP)* (A, C, E, G). Note the enhanced clustering of melanocytes in the posterior part of the dorsal head in treated embryos (blue arrows) ; the normal distribution in this area in untreated controls is indicated by red arrows. Heat shock activation of Wnt inhibition consistently resulted in smaller heads and eyes. Scale bars: 100 μm.

Supplemental data

Supplementary Figure 1: Ripley's K function analysis shows significant decrease in melanocyte organisation in BIO-treated embryos compared to DMSO-treated embryos at 72 hpf.
Ripley's K function analysis was performed on 10 DMSO treated embryos (A-J) and 10 BIO treated embryos (K-S). The expected values for K if the cells are randomly spread are represented by the red dotted line on the graph; the grey area corresponds to area between the lower and higher confidence envelope/interval for values of K. Based on inspection of control embryos, and noting that the dorsal head melanocytes are clearly patterned, we set the scale of analysis to r=35 pixels (blue arrows and blue lines). Significant clustering then corresponds to the white zone underneath the grey area whereas significant dispersion corresponds to the white area above the grey area. As expected, 8 out of 10 DMSO-treated control embryos are scored as showing a clustered pattern (below the grey area; embryos A-E,G,H,J). In contrast, Ripley's K function analysis performed on BIO treated embryos showed that the observed K values were found within the lower confidence envelope (in the grey area) of the graph in nine out of ten embryos (embryos K-S), so that cells appeared randomly dispersed in 90% of the cases.

Supplementary Figure 2: Strong expression of a dntcf3 transgene results in poor melanocyte differentiation. Transgenic *Tg(hsp70l:tcf3-deltaC-GFP)* embryos **t**hat were heat shocked at each of 29, 36, 48 and 62 hpf and which showed strong GFP expression (A,C,E) demonstrate a strong melanocyte phenotype including reduced melanisation and more rounded shape (red arrowheads) at 73 hpf compared to non-heat-shocked control transgenic embryos (B,D,F). Scale bars: 100 μm.

Supplemental Figure 3: Ripley's K function analysis shows significant decrease in melanocyte organisation when Wnt signalling is impaired in dntcf3 transgenic embryos at 72 hpf. Ripley's K function analysis was performed on 10 control non-heat-shocked transgenic *Tg(hsp70l:tcf3-deltaC-GFP)* embryos (A-J) and 10 heat-shocked transgenic *Tg(hsp70l:tcf3-deltaC-GFP)* embryos (K-T). The expected values for K if the cells are randomly spread are represented by the red dotted line on the graph; the grey area corresponds to area between the lower and the higher confidence envelope/interval for values of K. Based on inspection of control embryos, and noting that the dorsal head melanocytes are clearly patterned, we set the scale of analysis to r=50 pixels (blue arrows and blue lines). Significant clustering then corresponds to the white zone underneath the grey area whereas significant dispersion corresponds to the white area above the grey area. As expected, eight out of ten control embryos are scored as showing a clustered pattern (below the grey area; embryos A-E,G,H,J). In contrast, Ripley's K function analysis performed on heat-shocked embryos showed that the observed K values were found within the lower confidence envelope (in the grey area) of the graph in seven out of ten embryos (embryos K-S), so that cells showed 'lower organisation' in 70% of the cases.

Supplementary Figure 4:

A) Core GRN for melanocyte differentiation activated by Wnt signaling. Extension of Gene Regulatory Network as from Greenhill et al., (2011) with inclusion of β-catenin/Lef-1 (indicated in the diagram as T) mediated Wnt activation. The complex β-catenin/Lef-1 is assumed to work in conjunction with Sox10 and Mitfa through AND gates. Two components of Wnt signaling (WntA and WntB) are also assumed to participate selectively in fate specification and commitment respectively.

B) Schematic of WntA and WntB signaling.

We show the time profile of the Wnt components, WntA and WntB, as used in this model. The first component is active between times 15-30 hpf and activates production of nuclear T (plotted) above the threshold value while the second component is active for times beyond 30 hpf and has a lower affinity not enough to induce a production of T above threshold. Note that although modelled here as differences in affinity for their receptors, exactly equivalent outcomes would result if their affinities were identical, but WntA and WntB expression levels differed.

C-D) Selective failure of specification and commitment.

We plot the response of the GRN to either Wnt component acting alone. When only WntA is active (C) we have specification but only transient differentiation (Mitfa increases initially, but then decays to zero) while when only WntB is active (D) Mitfa production is never observed. The traces of Sox10 (red curve), Z (orange), T (blue), Dct (dark green), Tyrp1 (brown), A (black) and Mitfa (light green) are plotted as a function of time (hours after fertilisation, hpf).

E-F) Simulation of the core GRN according to the mathematical model (see Methods).
The traces of Sox10 (red curve), Z (orange), T (blue), Dct (dark green), Tyrp1 (brown), A (black) and Mitfa (light green) are plotted as a function of time (hrs). Solid lines correspond to time-courses without BIO treatment while circles correspond to those with BIO treatment. E) BIO treatment is applied between 24 and 48 hpf, Mitfa (light green circles) is amplified 2-fold at 48 hrs as compared to the evolution without BIO treatment (light green line) at the same time. F) BIO treatment is applied between 24 and 72 hpf, Mitfa (light green circles) is amplified 3-fold at 72 hrs as compared to the evolution without BIO treatment (light green line) at the same time.

Methods

Fish Husbandry

Wild type (AB) and transgenic *Tg(-7.2sox10:EGFP*) (Carney et al., 2006) and *Tg(top:GFP))* (Dorsky et al., 2002) and mutant *mitfa*^{w2} (Lister et al., 1999) zebrafish, *Danio rerio*, were kept in the aquarium at the University of Bath. *Tg(hsp70l:tcf3-deltaC-GFP) (*=w26Tg) fish (Martin and Kimelman, 2012) were kept in the facilities of the Department of Developmental and Cell Biology, School of Biological Sciences at the University of California, Irvine. Natural crosses were set up overnight and embryos collected in the morning. Embryos were placed in embryo medium and grown at 28.5 °C. They were staged according to Kimmel et al., (1995). Where embryos were to be manipulated between laying and hatching we used Watchmakers' No5 forceps to dechorionate the embryos. Embryos older than 15 hpf which were to be manipulated in any way were anaesthetised with Tricaine (Ethyl 3-aminobenzoate methanesulphonate, 4 g/L stock, final concentration approximately 0.2 % v/v). Where appropriate, melanisation was inhibited using PTU (1-phenyl-2-thiourea) from 24 hpf at a final concentration of 0.0015 % in embryo medium. All experiments complied with institutional and national animal welfare laws, guidelines and policies. Procedures involving fish older than 5 dpf were undertaken under licence from the UK Home Office.

BIO (2'*Z*,3'*E*)-6-Bromoindirubin-3'-oxime) treatment

BIO (2'*Z*,3'*E*)-6-Bromoindirubin-3'-oxime)*:* GSK3β inhibitor (Calbiochem) was stored as a 10 mM stock solution in DMSO. Ten wild type or *mitfa*^{w2} mutant embryos were placed in triplicate into 6-cm petri dishes containing 8 ml embryo medium. All embryos were dechorionated before 10 mM BIO

(361550 GSK-3 Inhibitor IX, Calbiochem) in DMSO was added to each experimental dish to a final concentration of 5 µM; an equivalent volume of DMSO was added to the control dishes. Embryos were incubated under standard conditions from 15-30, 24-48, 48-72 or 24-72 hpf.

Heat-shock experiment

Tg(hsp70l:tcf3-deltaC-GFP) transgenic embryos (Martin and Kimelman, 2012) were heat shocked at 39°C for 12 minutes at four timepoints (29 hpf, 36 hpf, 48 hpf and 60 hpf) during melanocyte differentiation; after heat-shock, embryos were assessed for GFP expression and left to develop at 28.8°C in incubator. Embryos were assessed for melanocyte differentiation defects at 73 hpf.

Whole mount *in situ* hybridisation

RNA *in situ* hybridisation was performed according to Thisse and Thisse, (2008) except probes were not hydrolysed and embryos were incubated at 68 °C in hybridization steps. Probes used were *sox10* (Dutton et al., 2001), *mitfa* (Lister et al., 1999), *xdh* (Parichy et al., 2000). (Plasmid and probe generated by T. Chipperfield and C. Nelson).

RNA extraction and cDNA synthesis

RNA was extracted from samples consisting of 50 whole embryos of each condition using TRI REAGENT (Sigma-Aldrich, T9424) according to manufacturer's instructions and purified and precipitated by phenol/chloroform/isoamylalcohol (25:24:1). The RNA pellet was washed in 1ml 75% ETOH by inverting the tube gently. A 1 µl sample was assessed for purity, integrity by gel electrophoresis, and concentration was measured spectrophotometrically. When required, samples were stored at -80°C for not more than a month. For experiment using WT embryos, first strand cDNA was synthesised using the Invitrogen First strand cDNA synthesis kit with Superscript III and oligodT (Promega), 0.5 µl random hexamers (250ng/µl) (Promega), 5 µl dNTPs (2mM) (Promega), 7.5 µl RNA (1 µg of total RNA) were first mixed and incubated for 5 mins at 65^{o}C and then at least 1 min at 4^{o}C. Second, 4 µl of 5X first strand buffer (Invitrogen), 1 µl of 5mM DTT, 1 µl RNAse out (Invitrogen) and 1 µl superscript III (Invitrogen) RTase/Mµl were added to the previous mix and left 5 minutes at 25 ^{o}C, 60 ^{o}C minutes at 50 ^{o}C, 15 minutes at 70 ^{o}C. Finally, samples were diluted 1:5 and concentrations were measured spectrophotometrically. For experiments using mitfa^{w2} mutant embryos, RNA extraction was performed by Direct-zol™ RNA MiniPrep (Zymo Research) and the iScript™ Advanced cDNA Synthesis Kit (Bio-Rad) was used for reverse transcription of 1 µg RNA in 20 µl reaction according to manufacturer's protocol.

Real-time quantitative PCR

.Real time quantitative PCR was performed in triplicate using SYBR Green I PCR Master Mix (Roche) for WT embryos and a Lightcycler II machine (Roche) was used according to the manufacturer's instructions. For *mitfa*^{w2} mutant embryos, the Fast SYBR® Green Master Mix (ThermoFisher) was used and samples were run in triplicate using the StepOne™ System (ThermoFisher) according to manufacturer's instructions. Standard curves for both *gapdh* and *mitfa* primers demonstrated nearly 100% efficiency (98.7% and 98.5%, correspondently). Primers were designed spanning an intron using Primer3 Plus software (http://www.bioinformatics.nl/cgibin/primer3plus/primer3plus.cgi.). The following primers were used:

gapdh: forward 5'ACCAACTGCCTGGCTCCT3',
reverse 5'TACTTTGCCTACAGCCTTGG3';

mitfa: forward 5'CTGGACCATGTGGCAAGTTT3',
reverse 5'GAGGTTGTGGTTGTCCTTCT3'

Gene expression was normalized against zebrafish *gapdh* expression in wild-type embryos. RT-qPCR data were analysed using the (ΔΔCt) method (Livak et al., 1998). Student's t-test was performed using GraphPadPrism 5.0. In all tests, difference was considered significant if $p<0.001$.

Immunofluorescence

Embryos for immunofluorescent detection were processed following the protocol proposed by (Ungos et al., 2003). Embryos were fixed in 4 % Paraformaldehyde in PBS (Phosphate buffered saline, Oxoid) overnight at 4 °C. They were washed three times for 5 minutes in PBTriton (0.1 % Triton X-100 Sigma-Aldrich in PBS) and three times for one hour in MilliQ water. Embryos were incubated in block solution (1 % DMSO, 5 % Goat/Sheep serum diluted in PBTriton) for 2 to 3 hours. They were then incubated at room temperature overnight in polyclonal mouse serum primary antibody (Polyclonal IgG Rabbit Anti-GFP Primary Antibody, Invitrogen, A11122) diluted 1:500 in block solution. Embryos were washed in PBTriton once briefly and three times for one hour. They were incubated overnight 4 °C in Alexa Fluor 488 fluorescent anti-rabbit secondary antibody (Polyclonal IgG Alexa Fluor 488 donkey anti-rabbit, Invitrogen, A21206) diluted 1:200 in block solution. Embryos were then washed once briefly and three times for 30 minutes in PBTriton. They were stored in 50 % glycerol for imaging and storage.

Microscopy

Fish were mounted between bridged coverslips in methylcellulose for live embryos, anesthetized with 0.003 % MS222 (Sigma), and in 80 % glycerol for fixed embryos. Embryos were photographed using a Spot digital camera (supplier) mounted on an Eclipse E800 microscope (Nikon) or Axioplan 2 microscope (Zeiss) with DIC optics using a Spot digital camera mounted on a MZ12 microscope (Leica) with epi-illumination or Nikon sight DS-U1 camera (Nikon). To minimise the effects of the

developmental gradient along the body axis, melanocyte counts were performed on the head only, from the anteriormost region (forebrain) to the rear of the otic vesicle (posterior hindbrain); melanocytes were counted only in the region dorsal to the CNS (i.e the developing dorsal stripe).

Dendricity measurement

Dendricity was calculated as **R** *(R = P2/4pA, where A is the cell area and P the cell perimeter),* cell perimeter and area was measured using ImageJ software from images of cells taken using Eclipse E800 microscope (Nikon).

Ripley's K function analysis

To quantify and compare melanocyte organisation in DMSO treated embryos and BIO treated embryos the Multi-Distance Spatial Cluster Analysis, based on Ripley's K-Function, was performed using R statistical software (using packages "spatstat" and "dplyr" (R Core Team (2012)). Melanocyte positions were determined on the dorsal head of ten treated 72 hpf embryos for each conditions (DMSO and BIO treated) using comparable pictures. x and y coordinates for each melanocyte's position was determined using ImageJ. This data was then used to perform the Ripley's K function analysis which allows testing for random partition of the cells.

A Z-test allowed comparison of the two populations for cellular spatial organisation using the results of this analysis; the result was considered significant if $p<0.01$.

Statistics

Data were analysed by Prism 3.0 software GraphPadPrism 5.0 using unpaired t-test, $\alpha=0.05\%$, $n=20$ and $fd= (x-2)$, with x = number of embryo tested.

Mathematical Modelling

Following the scheme of Supp. Fig. 3A and indicating the molecular species with their initials (except Tyrp1, indicated with T_y) we describe the behaviour of the GRN by the following set of ordinary differential equations:

$$\frac{dZ}{dt} = g_Z \frac{B}{K_B + B} - d_Z Z$$

$$\frac{dS}{dt} = g_S \left[\frac{\Phi_2 A(\Omega_1\Omega_2 + \Omega_1 H) + \Omega_2 M(\Phi_1\Phi_2 + \Phi_1 H) + \Omega_2 M\Phi_2 A}{(\Phi_1\Phi_2 + \Phi_2 A + \Phi_1 H)(\Omega_1\Omega_2 + \Omega_2 M + \Omega_1 H)} \right] - d_S S$$

$$\frac{dM}{dt} = g_M \left[\frac{(\Gamma_2 S + \Gamma_1 S^2)\widetilde{T}}{(\Gamma_{12} + \Gamma_2 S + \Gamma_1 S^2)(K_T + \widetilde{T})} \left(1 - \frac{\widetilde{M}T}{(K_T + T)(K_M + \widetilde{M})} \right) + \frac{\widetilde{M}\widetilde{T}}{(K_T + \widetilde{T})(K_M + \widetilde{M})} \right] - d_M M$$

$$\frac{dT}{dt} = g_T \frac{K_{WB} W_A(t) + K_{WA} W_B(t) + W_A(t) W_B(t)}{(K_{WB} + W_B(t))(K_{WA} + W_A(t))} - d_T T$$

$$\frac{dH}{dt} = g_H \frac{M}{K_{M1} + M} - d_H H$$

$$\frac{dT_y}{dt} = g_{Ty} \frac{M}{K_{M2} + M} - d_{Ty} T_y$$

$$\frac{dD}{dt} = g_D \frac{K_Z M + K_{M3} Z + MZ}{(K_Z + Z)(K_{M3} + M)} \frac{K_S}{K_S + S} - d_D D$$

$$\text{with : } \begin{cases} \widetilde{M} = M\Theta(M - \overline{M}) \\ \widetilde{T} = T\Theta(T - \overline{T}) \end{cases}, \quad \begin{cases} W_A(t) = W_A\left(\Theta(t - 30h) - \Theta(t - 15h)\right) G_{BIO} \\ W_B(t) = W_B \Theta(t - 30h) G_{BIO} \end{cases}$$

$$\text{and : } \Theta(x) = \begin{cases} 0 & x < 0 \\ 1 & x \geq 0 \end{cases}, \quad G_{BIO} = \begin{cases} 1 & \text{untreated} \\ (t - t^S_{BIO})\left(\Theta(t - t^E_{BIO}) - \Theta(t - t^S_{BIO})\right) & \text{BIO - treated} \end{cases}$$

All equations have been derived from the network scheme in Supp. Fig. 3A by applying the rules explained in Greenhill et al. (2011). In addition, here we consider β-catenin/Lef-1 (T) acting in conjunction with either Sox10 (S) or Mitfa (M) via an AND gate in order to activate the production of Mitfa itself. This means that Mitfa production is activated only when either of the two AND gates involving T (one with Sox10 and the other with Mitfa) is active. The AND gate with Sox10 is activated only when the concentration of T is larger than a given threshold $\overline{T}$. A second threshold $\overline{M}$ on the concentration of Mitfa is operative also on the self-activating loop of Mitfa.

The core of the network corresponds to what has already been modelled in Greenhill et al. (2011) with the addition of Wnt signaling. Wnt is assumed to have two components WntA (W_A in the equations above) and WntB (W_B) both activating transcription factor β-catenin/Lef-1 (indicated as T in the equations). The binding and unbinding dynamics of Wnt is assumed to be fast as compared to the other network reactions and therefore Wnt is assumed to be equilibrated at any time. The first component WntA is present only for a transient time between 15 and 30 hpf, while the second component WntB starts at 30 hpf and remains active throughout the whole differentiation process (see Supp. Fig. 3B). When these two components act together they guarantee specification and commitment of the melanocytes lineage. If only WntA is present then we have specification but no commitment (see Supp. Fig. 3C) while if only WntB is present no specification is observed (Supp. Fig. 3D). Notice that this mechanism relies on the presence of a threshold on the activation of the

AND gate between Sox10 and T which prevents the production of Mitfa and therefore the activation of Mitfa's feedback loop. In order to simulate the BIO-treatment we added a correction G_{BIO} to the W_A and W_B components, which amounts to a time-linear increase in Wnt when the BIO-treatment is applied between t^S_{BIO} and t^E_{BIO} (times of start and end of the treatment respectively) and is one when there is no BIO-treatment. Parameter values for the model are:

$$\begin{cases} g_Z = 0.1\,\text{nM/h} \\ g_S = 0.3\,\text{nM/h}, \\ g_M = 0.35\,\text{nM/h} \\ g_T = 1.3\,\text{nM/h} \\ g_H = 0.3\,\text{nM/h} \\ g_{Ty} = 3.1\,\text{nM/h} \\ g_D = 0.3\,\text{nM/h} \end{cases}, \quad \begin{cases} d_Z = 0.2\,\text{h}^{-1} \\ d_S = 0.3\,\text{h}^{-1} \\ d_M = 0.05\,\text{h}^{-1} \\ d_T = 0.6\,\text{h}^{-1} \\ d_H = 0.03\,\text{h}^{-1} \\ d_{Ty} = 0.6\,\text{h}^{-1} \\ d_D = 0.1\,\text{h}^{-1} \end{cases}, \quad \begin{cases} \Omega_1 = 1.92\,\text{nM} \\ \Omega_2 = 1.43\,\text{nM} \\ \Omega_{12} = 1.32\,\text{nM} \\ \Phi_1 = 2.0\,\text{nM} \\ \Phi_2 = 0.22\,\text{nM} \\ \Phi_{12} = 0.1\,\text{nM} \\ K_B = 0.175\,\text{nM} \\ K_{WA} = 0.5\,\text{nM}, \\ K_{WB} = 0.5\,\text{nM} \end{cases}, \quad \begin{cases} K_T = 7.8\,\text{nM} \\ K_M = 0.045\,\text{nM} \\ K_{M1} = 1.0\,\text{nM} \\ K_{M2} = 1.8\,\text{nM} \\ K_{M3} = 1.0\,\text{nM} \\ K_Z = 6.5\,\text{nM} \\ K_S = 1.2\,\text{nM} \end{cases}, \quad \begin{cases} W_A = 0.33\,\text{nM} \\ W_B = 0.25\,\text{nM} \\ \overline{M} = 0.01\,\text{nM}, \\ \overline{T} = 0.75\,\text{nM} \\ \Gamma_1 = 5.0\,(\text{nM}\cdot\text{h})^{-2} \\ \Gamma_2 = 4.5\,(\text{nM}\cdot\text{h})^{-2} \\ \Gamma_{12} = 1.8\,(\text{nM}\cdot\text{h})^{-2} \end{cases}$$

These values are chosen in accordance with measured values from the literature (Jin & Liao, 1999, Schwanhausser et al., 2011 and Eden et al., 2011 for Sox10, Jao et al., 2013 for Mitfa) and within similar ranges as in Greenhill et al. (2011) for those unknown. We have assumed the same affinity for the two Wnt components and larger concentration for W_A but the opposite assumption (different affinity and same concentration) would lead to the same results. A slower decay rate for Mitfa than the one used in Greenhill et al., 2011 produced a better quantitative agreement with BIO-treatment results.

Acknowledgements

We gratefully acknowledge M. Welham for provision of BIO stock for preliminary experiments in this study, S. Wilson for supplying the *Tg(top:GFP)* fish, N. Parkinson and Robert J. Burnside for technical advice, and H. Schwetlick and S. Mulnoz-Descalzo for helpful comments on the manuscript. Funding was provided by University of Bath Graduate Studentship (LV), and BBSRC grant BB/L00769X/1 (RNK) and BBSRC grant BB/L007789/1 (GA and AR), as well as NIH R01 DE013828 (TFS).

Alexander, C., Piloto, S., Le Pabic, P.,Schilling, TF. (2014), Wnt signalling interacts with bmp and edn1 to regulate dorso-ventral patterning and growth of the craniofacial skeleton. PLoS Genet, 7, e1004479

Aoude, AG.,Wadt, KA., Pritchard, AL., Hayward, N.K. (2015), Genetics of familial melanoma: 20 years after CDKN2A. Pigment Cell Melanoma Res, *28(2)*, 148-60.

Baddeley, A. and Turner,R . (2005). spatstat: An R Package for Analyzing Spatial Point Patterns. Journal of Statistical Software 12(6), 1-42.

Barker, N. (2008), The canonical Wnt/beta-catenin signaling pathway. Methods Mol Biol*, 468***,** 5-15.

Bellei, B., Flori, E., Izzo, E., Maresca, V. & Picardo, M. (2008), GSK3beta inhibition promotes melanogenesis in mouse B16 melanoma cells and normal human melanocytes. Cell Signal*, 20***,** 1750-61.

Bellei, B., Pitisci, A., Catricala, C., Larue, L. & Picardo, M. (2010), Wnt/beta-catenin signaling is stimulated by alpha-melanocyte-stimulating hormone in melanoma and melanocyte cells: implication in cell differentiation. Pigment Cell Melanoma Res*, 24***,** 309-25.

Carney, T. J., Dutton, K. A., Greenhill., E., Delfino-Machin, M., Dufourcq, P., Blader, P. & Kelsh, R. N. (2006), A direct role for Sox10 in specification of neural crest-derived sensory neurons. Development*, 133***,** 4619-30.

Cheli, Y., Ohanna, M., Balloti R. & Bertolotto, C. (2012), Fifteen-year quest for microphthalmia-associated transcription factor target genes. Pigment Cell Melanoma Res*, 23***,** 27-40.

Curran, K., Lister, J. A., Kunkel, G. R., Prendergast, A., Parichy, D. M. & Raible, D. W. (2010), Interplay between Foxd3 and Mitf regulates cell fate plasticity in the zebrafish neural crest. Dev Biol*, 344***,** 107-18.

Dorsky, R. I., Moon, R. T. & Raible, D. W. (1998), Control of neural crest cell fate by the Wnt signaling pathway. Nature*, 396***,** 370-3.

Dorsky, R. I., Moon, R. T. & Raible, D. W. (2000), Environmental signals and cell fate specification in premigratory neural crest. Bioessays*, 22***,** 708-16.

Dorsky, R. I., Sheldahl, L. C. & Moon, R. T. (2002), A transgenic Lef1/beta-catenin-dependent reporter is expressed in spatially restricted domains throughout zebrafish development. Dev Biol*, 241***,** 229-37.

Dunn, K. J., B. O. Williams, Y. Li and W. J. Pavan. (2000), Neural crest-directed gene transfer demonstrates Wnt1 role in melanocyte expansion and differentiation during mouse development. Proc Natl Acad Sci U S A **97**(18): 10050-10055.

Dutton, K. A., Pauliny, A., Lopes, S. S., Elworthy, S., Carney, T. J., Rauch, J., Geisler, R., Haffter, P. & Kelsh, R. N. (2001), Zebrafish colourless encodes sox10 and specifies non-ectomesenchymal neural crest fates. Development, *128*, 4113-25.

Eden, E., Geva-Zatorsky, N., Issaeva, I., Cohen, A., Dekel, E., Danon, T., Cohen, L., Mayo, A., Alon, U. (2011) Proteome half-life dynamics in living human cells. Science, *331*, 764-8.

Greenhill, E. R., Rocco, A., Vibert, L., Nikaido, M. & Kelsh, R. N. (2011), An iterative genetic and dynamical modelling approach identifies novel features of the gene regulatory network underlying melanocyte development. PLoS Genet, *7*, e1002265.

Hari, L., Miescher, I., Shakhova, O., Suter, U., Chin, L., Taketo, M., Richardson, W. D., Kessaris, N. & Sommer, L. (2012), Temporal control of neural crest lineage generation by Wnt/beta-catenin signaling. Development, *139*, 2107-17.

Herbarth, B., Pingault, V., Bondurand, N., Kuhlbrodt, K., Hermans-Bormeyer, I., Puliti, A., Lemort, N., Goossens, M., Wegner, M. (1998), Mutation of the Sry-related Sox10 gene in Dominant megacolon, a mouse model for human Hirschsprung disease. Proc Natl Acad Sci U S A, *95*, 5161-5.

Hodgkinson, C. A., Moore, K. J., Nakayama, A., Steingrimsson, E., Copeland, N. G., Jenkins, N. A. & Arnheiter, H. (1993), Mutations at the mouse microphthalmia locus are associated with defects in a gene encoding a novel basic-helix-loop-helix-zipper protein. Cell, *74*, 395-404.

Ikeya, M., Lee, S. M., Johnson, J. E., McMahon, A. P. & Takada, S. (1997), Wnt signaling required for expansion of neural crest and CNS progenitors. Nature, *389*, 966-70.

Jao, Le., Wente, SR., Chen, W. (2013) Efficient multiplex biallelic zebrafish genome editing using a CRISPR nuclease system. Proc Natl Acad Sci U S A,*110*, 13904-9.

Jin, E. J. & Thibaudeau, G. (1999), Effects of lithium on pigmentation in the embryonic zebrafish (Brachydanio rerio). Biochim Biophys Acta, *1449*, 93-9.

Jin, C & Liao, X. (1999), Backbone dynamics of a winged helix protein and its DNA complex at different temperatures: changes of internal motions in genesis upon binding to DNA. J Mol Bio *292*, 641-51.

Jonhson, S.L., Nguyen, A.N., Lister, J.A. (2011), mitfa is required at multiple stages of melanocyte differentiation but not to establish the melanocyte stem cell. Dev Biol. *350*, 405-413.

Kaufman, C.K., Mosimann, C., Fan, Z.P., Yang, S., Thomas, AJ., Ablain, J, Tan, J.L., Fogley, R.D., Van Rooijen, E., Hagedom, E.J., Ciarlo, C., White, R.M., Matos, D.A., Puller, A.C., Santeriello, C., Liao, EC., Young, R.A., Zon, L.I. (2016), A zebrafish melanoma model reveals emergence of neural crest identity during melanoma initiation. Science, *351,* 6272.

Kawasaki, A., Kumasaka, M., Satoh, A., Suzuki, M., Tamura, K., Goto, T., Asashima, M. & Yamamoto, H. (2008), Mitf contributes to melanosome distribution and melanophore dendricity. Pigment Cell Melanoma Res, *21*, 56-62.

Kelsh, R. N. (2006), Sorting out Sox10 functions in neural crest development. Bioessays, *28*, 788-98.

Kim, J. H., Sohn, K. C., Choi, T. Y., Kim, M. Y., Ando, H., Choi, S. J., Kim, S., Lee, Y. H., Lee, J. H., Kim, C. D. (2010), Beta-catenin regulates melanocyte dendricity through the modulation of PKCzeta and PKCdelta. Pigment Cell Melanoma Res, *23*, 385-93.

Kimmel, C. B., Ballard, W. W., Kimmel, S. R., Ullmann, B. & Schilling, T. F. (1995), Stages of embryonic development of the zebrafish. Dev Dyn, *203*, 253-310.

Korinek, V., Barker, N., Morin, P. J., Van Wichen, D., De Weger, R., Kinzler, K. W., Vogelstein, B. & Clevers, H. (1997), Constitutive transcriptional activation by a beta-catenin-Tcf complex in APC-/- colon carcinoma. Science, *275*, 1784-7.

Kumasaka, M., Sato, S., Yajima, I., Goding, C. R. & Yamamoto, H. (2005), Regulation of melanoblast and retinal pigment epithelium development by Xenopus laevis Mitf. Dev Dyn, *234*, 523-34.

Lee, H. Y., M. Kleber, L. Hari, V. Brault, U. Suter, M. M. Taketo, R. Kemler and L, Sommer. (2004), Instructive role of Wnt/beta-catenin in sensory fate specification in neural crest stem cells. Science, *303*, 1020-1023.

Lee, M., Goodall, J., Verastegui, C., Ballotti, R. & Goding, C. R. (2000), Direct regulation of the Microphthalmia promoter by Sox10 links Waardenburg-Shah syndrome (WS4)-associated hypopigmentation and deafness to WS2. J Biol Chem, *275*, 37978-83.

Levy, C., Khaled, M., Fisher, D.E. (2006), MITF: master regulator of melanocyte development and melanoma oncogene. Trends Mol Med., *12*, 406-14.

Lewis, J. L., Bonner, J., Modrell, M., Ragland, J. W., Moon, R. T., Dorsky, R. I. & Raible, D. W. (2004), Reiterated Wnt signaling during zebrafish neural crest development, Development, *131*, 1299-308.

Lister, J. A., Robertson, C. P., Lepage, T., Johnson, S. L. & Raible, D. W. (1999), nacre encodes a zebrafish microphthalmia-related protein that regulates neural-crest-derived pigment cell fate. Development, *126*, 3757-67.

Livak, K. J., Little, W. A., Stack, S. L. & Patterson, T. A. (1998), Polymorphisms in the human DNA ligase I gene (LIG1) including a complex GT repeat. Mutat Res, *406*, 1-8.

Martin, B.L, & Kimelman, D. (2012). Canonical Wnt signalling dynamically controls multiple stem cell decisions during vertebrate body formation. Dev. Cell 22, 223-232.

Moro, E., Ozhan-Kizil, G., Mongera, A., Beis, D., Wierzbicki, C., Young, RM., Bournele, D., Domenichini, A., Valdivia, L.E., Lum, L., Chen, C., Amatruda, J.F., Tiso N,Weidinger, G., Argenton, F. (2012), In vivo Wnt signaling tracing through a transgenic biosensor fish reveals novel activity domains. Developmental Biology, 366(2):327-40.

Mort, RL., Jackson, LJ., Patton, EE. (2015), The melanocyte lineage in development and disease. Development, *142*, 1387

Novak, A. & Dedhar, S. (1999), Signaling through beta-catenin and Lef/Tcf. Cell Mol Life Sci, *56*, 523-37.

Opdecamp, K., Nakayama, A., Nguyen, MT., Hodgkinson, C.A., Pavan, WJ, Arnheiter, H. (1997), Melanocyte development in vivo and in neural crest cell cultures: crucial dependence on the Mitf basic-helix-loop-helix-zipper transcription factor. Development, *124*, 2377-86.

Parichy, D. M., Ransom, D. G., Paw, B., Zon, L. I. & Johnson, S. L. (2000), An orthologue of the kit-related gene fms is required for development of neural crest-derived xanthophores and a subpopulation of adult melanocytes in the zebrafish, Danio rerio. Development*, 127***,** 3031-44.

Price, L. H. & Heninger, G. R. (1994), Lithium in the treatment of mood disorders. N Engl J Med*, 331***,** 591-8.

R Core Team (2012). R: A language and environment for statistical computing. R Foundation for Statistical Computing, Vienna, Austria. ISBN 3-900051-07-0

Ripley, B.D. (1977) Modelling spatial patterns (with discussion). *Journal of the Royal Statistical Society, Series B*, **39**, 172 – 212.

Schwanhäusser, B., Busse, D., Li, N., Dittmar, G., Schuchhardt, J., Wolf, J., Chen, W., Selbach, M. (2011), Global quantification of mammalian gene expression control, Nature *473*, 337-342.

Sineva, G. S. & Pospelov, V. A. (2010), Inhibition of GSK3beta enhances both adhesive and signaling activities of beta-catenin in mouse embryonic stem cells. Biol Cell*, 102***,** 549-60.

Speeckaert, R., Speeckaert, M.M., Van Geel, N. (2015), Why treatments do(n't) work in vitiligo: An autoinflammatory perspective. Autoimmun Rev, *14*, 332-40.

Steingrimsson, E., Copeland, N. G. & Jenkins, N. A. (2004), Melanocytes and the microphthalmia transcription factor network. Annu Rev Genet*, 38***,** 365-411.

Takeda, K., Yasumoto, K., Takada, R., Takada, S., Watanabe, K., Udono, T., Saito, H., Takahashi, K. & Shibahara, S. (2000), Induction of melanocyte-specific microphthalmia-associated transcription factor by Wnt-3a. J Biol Chem*, 275***,** 14013-6.

Thisse, C. & Thisse, B. (2008), High-resolution in situ hybridization to whole-mount zebrafish embryos. Nat Protoc*, 3***,** 59-69.

Tseng, A. S., Engel, F. B. & Keating, M. T. (2006), The GSK-3 inhibitor BIO promotes proliferation in mammalian cardiomyocytes. Chem Biol*, 13***,** 957-63.

Uong, A. & Zon, L. I. (2009), Melanocytes in development and cancer. J Cell Physiol*, 222***,** 38-41.

Van De Wetering, M., Cavallo, R., Dooijes, D., Van Beest, M., Van E.S, J., Loureiro, J., Ypma, A., Hursh, D., Jones, T., Bejsovec, A. (1997), Armadillo coactivates transcription driven by the product of the Drosophila segment polarity gene dTCF. Cell*, 88***,** 789-99.

Van Otterloo E., Li, W., Bonde, G., Day, K.M., Hsu, M-Y., Cornell, R.A. (2010), Differentiation of Zebrafish Melanophores Depends on Transcription Factors AP2 Alpha and AP2 Epsilon. PLoS Genet. *16*, e1001122.

Watanabe, K., Takeda, K., Yasumoto, K., Udono, T., Saito, H., Ikeda, K., Takasaka, T., Takahashi, K., Kobayashi, T., Tachibana, M. (2002), Identification of a distal enhancer for the melanocyte-specific promoter of the MITF gene. Pigment Cell Res*, 15***,** 201-11.

White, R.M., Cech, J., Ratanasirintrawoot, S., Lin, CY., Rahl, P.B., Burke, C.J., Langdon, E., Tomlinson, M.L., Mosher, J., Kaufman, C., Chen, F., Long, H.K., Kramer, M., Datta, S., Neuberg, D., Granter, S., Young, R.A., Morrison, S., Wheeler, G.N., Zon, LI. (2011), DHODH modulates transcriptional elongation in the neural crest and melanoma, Nature 471, 518-22.

Yamaguchi, Y. and V. J. Hearing. (2014). Melanocytes and their diseases. Cold Spring Harb Perspect Med 4(5).

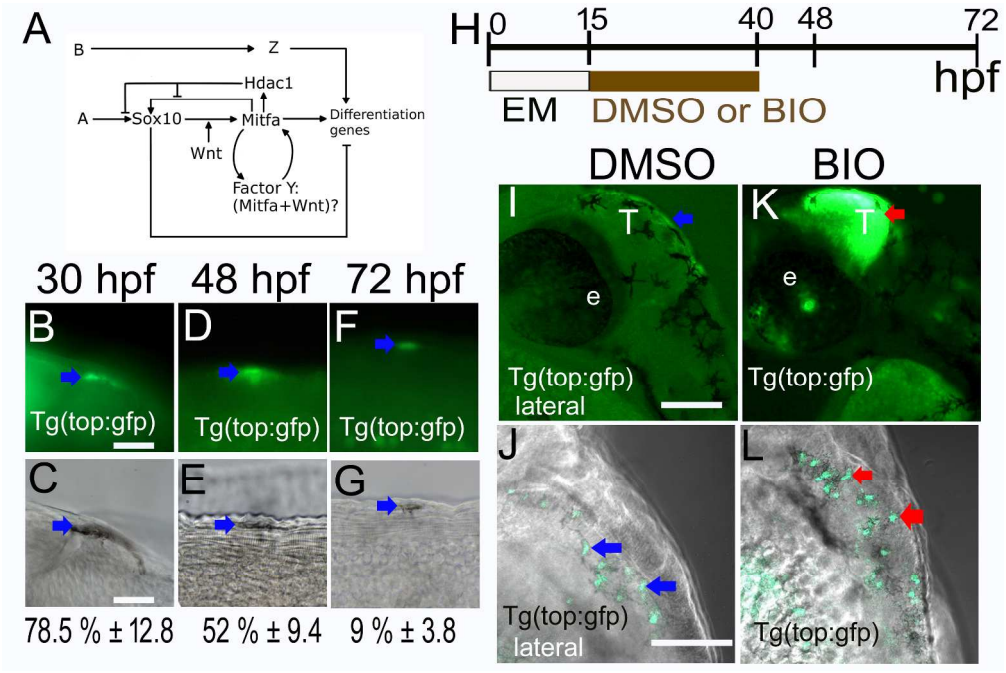

Figure 1.
Ongoing Wnt signaling is detectable in differentiating melanocytes.
(A) Diagram of working model for melanocyte core GRN (modified from Greenhill et al., 2011). Note two inputs from Wnt signaling on mitfa expression, one well-established role acting alongside Sox10 driving melanocyte fate specification, and hypothetical role explored here as part of a positive feedback loop also involving Mitfa itself. B-G) Wnt signaling in differentiating melanocytes was assessed by scoring samples of melanocytes for detection of dGFP by immunofluorescence in Tg(top:GFP) transgenic embryos from 30-72 hpf. GFP-positive melanocytes (arrows) are shown by immunofluorescence (B,D,F) and DIC (C,E,G) to show melanin pigment. At each stage, 30 melanocytes in each of 15 embryos were assessed for GFP expression, in the dorsal head and throughout the dorsal and lateral trunk; numbers show the percentage of melanocytes expressing GFP (mean ± s.d) at corresponding stages (n = 450 per stage). H) Schematic showing timing of BIO treatment used. I-L) BIO-treatment enhances activity of Tg(top:GFP) reporter. BIO-treatment from 15 hpf to 40 hpf dramatically enhances dGFP expression (red arrows) in the tectum of treated (K) compared with mock-treated controls (I) and also increases dGFP signal in melanocytes of Tg(top:GFP) embryos (BIO-treated (L) compared with mock-treated control (J)). All images, lateral views using confocal microscopy. EM, embryo medium; e: eye; T: tectum. Scale bars: B-G) 10 μm; I-L) 100 μm.

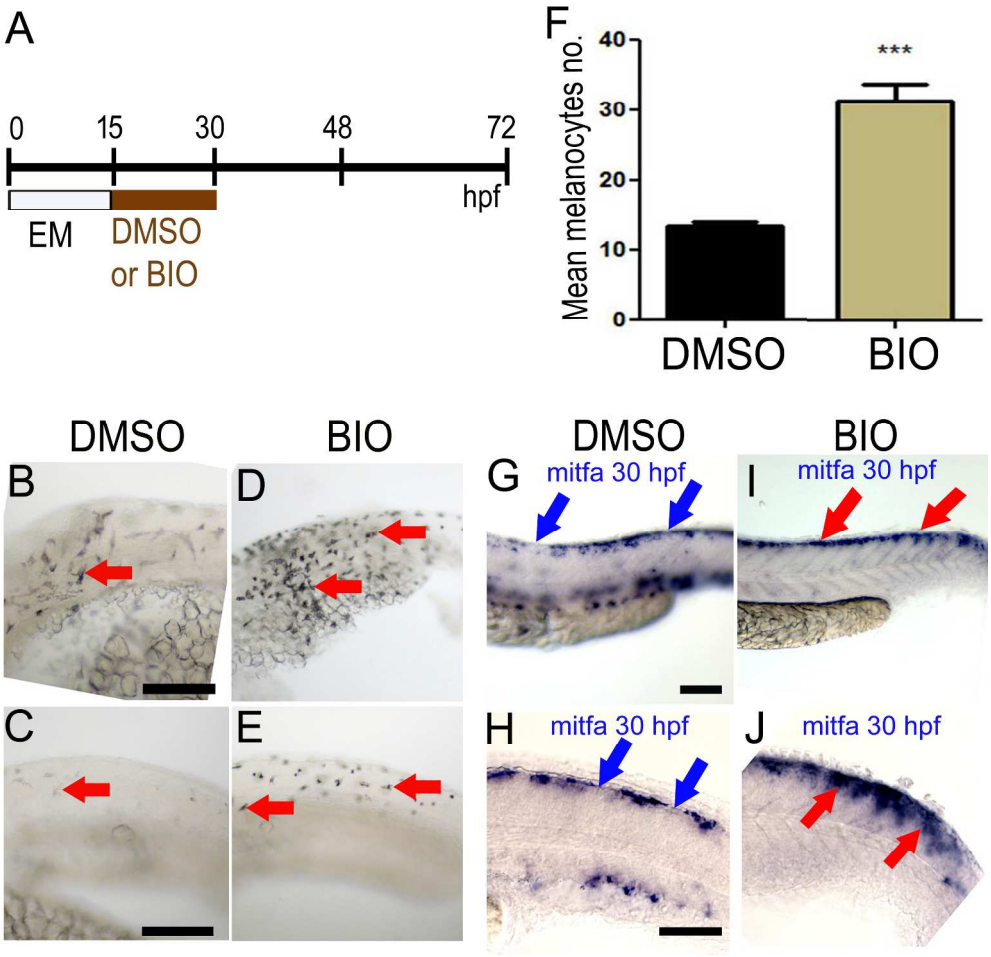

Figure 2. Elevated Wnt signaling in melanocyte specification time window increased numbers of melanocytes. A) Schematic showing timing of BIO treatment or control mock-treatment (DMSO alone) used. B-E) Lateral views of the trunk of live 30 hpf zebrafish embryos showing melanocytes (red arrows); note increased number in both anterior (D) and posterior trunk (E) of embryos treated with 5 μM BIO compared with control DMSO treated embryos (B,C respectively). F) Quantitation of increased melanocyte number in heads of BIO-treated embryos (mean ± s.d.; control, 13 ± 2.1; BIO, 32 ± 5.3, $p<10-6$) (n= 20; *** indicates significant difference between treated and mock-treated; unpaired, one-tailed t-test). G-J). Lateral views of posterior trunk (G,I) and close-up of anterior tail (H,J) of 30 hpf zebrafish embryo in situ hybridisations to show mitfa expression in embryos treated with BIO (I,J) or DMSO control (G,H). In the DMSO control embryos (G,H) discontinuous mitfa expression is observed in the dorsal region (blue arrows show discontinuities of the signal), whereas in the BIO treated embryos (I,J) mitfa expression is continuous throughout the dorsal region (red arrows). Images show representative phenotypes (n=20 per treatment). Scale bar: 100 μm.

Figure 2
240x231mm (299 x 299 DPI)

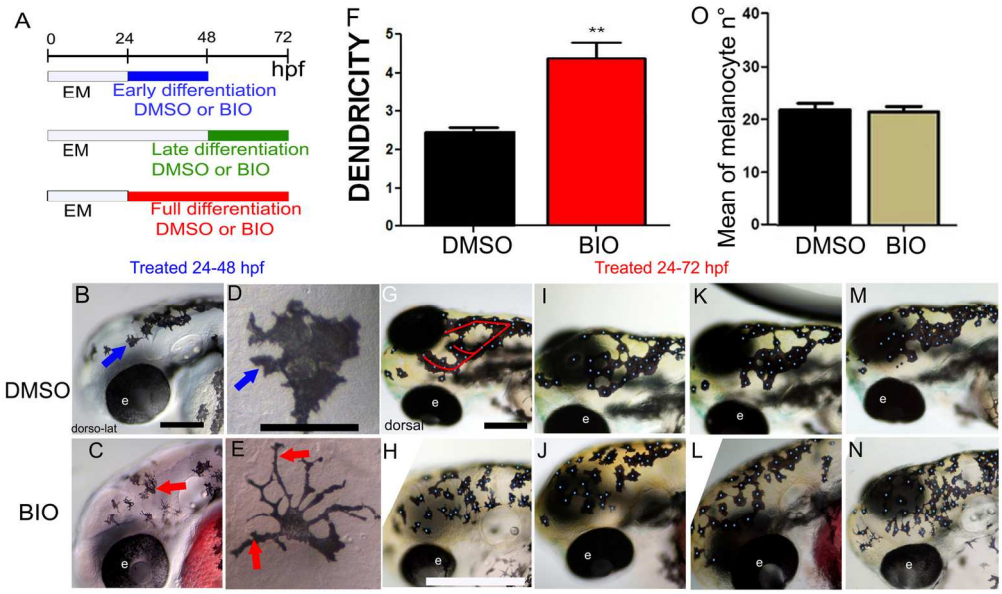

Figure 3: Elevated Wnt signaling in melanocyte differentiation time window alters melanocyte morphology. A) Schematic of melanocyte differentiation BIO-treatment time-windows. B-E) Activation of Wnt signaling in early differentiation period (24-48 hpf) increases melanocyte dendricity and dispersion. Lateral view at 48 hpf of head of live embryos treated with control DMSO (B) or BIO (C) from 24-48 hpf. Panels D and E show enlargements of head melanocytes from embryos in B and C respectively. F) Quantitation of dendricity: the cell roundness parameter was calculated for each melanocyte as $R = P2 / 4\prod A$, where A is the cell area and P the cell perimeter, 20 cells were investigated (n=20) in 10 different embryos for each condition. A score of R=1.0 represents a perfectly round melanocyte; increased R values represent increased dendricity. Control, R=2.44 ± 0.43, BIO R= 4.25 ± 1.68, p = 0.004, t-test result, p-value<0.01 (**). G-J) Elevated Wnt signaling throughout full differentiation or during late differentiation window only affects melanocyte organisation. Red line in G indicates the dorsal head melanophores which usually approximate an O- or U-shaped pattern, although often with extra branches as in this specific example. Dorsolateral view at 72 hpf of heads of live embryos treated with control DMSO (G,I,K,M) or BIO (H,J,L,N) from 24-72 hpf shown. Note that embryos treated in only Late Differentiation window (48-72 hpf) show equivalent phenotype (data not shown). Embryos shown are representative of samples examined (n=160 zebrafish embryos for each treatment). Scale bars: 100 µm (B,D,G,I).

149x93mm (300 x 300 DPI)

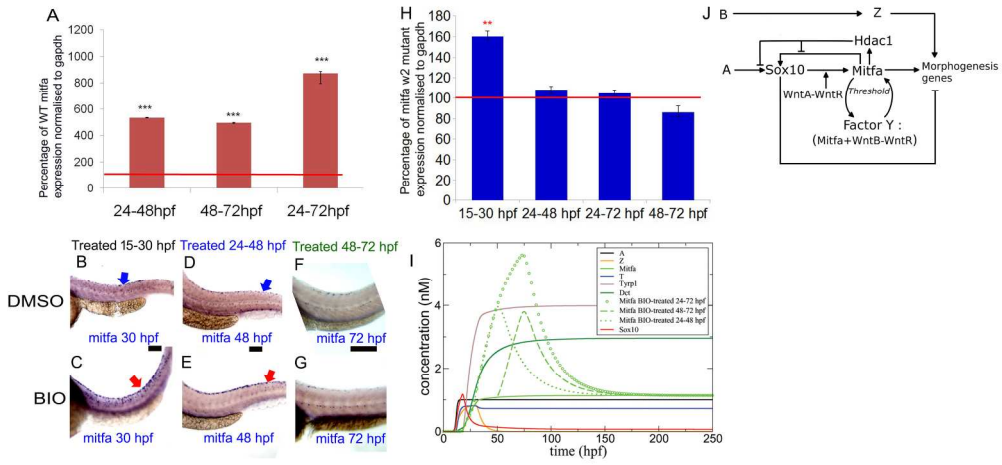

Figure 4: Positive feedback between Wnt signaling and Mitfa during late differentiation phase of melanocyte development. A) Quantitation of mitfa expression by RT-qPCR showing significantly increased levels in BIO-treated embryos compared with untreated controls; data are expressed as percentage of mock-treated controls (control mitfa level = 100 % transcripts (red line on graph)). Gene expression was investigated in 10 samples consisting of the trunk and tail of 50 embryos for each condition and in triplicate, after normalisation to the stable expression of a reference house-keeping gene, gapdh. All treatments caused significant increase of mitfa expression (t-test, two- tailed: 24-48 hpf, 535±7.1 (p= 0.00087); 48-72 hpf, 496±9.8(p= 0.0085); 24-72 hpf, 872±32.1 (p = 0.000092). ***, p-value<0.001). B-G) Activating Wnt signaling after 48 hpf does not affect mitfa expression in mitfaw2 mutant embryos during melanocyte differentiation. Lateral views of trunk showing in situ hybridisation for mitfa expression in mitfa mutant fish. mitfa mutant embryos treated with BIO in the melanocyte specification phase (15-30 hpf) (C) showed increased mitfa expression (purple) compared to DMSO-treated embryos (B). Similarly, mitfa mutant embryos treated with BIO in the melanocyte early differentiation phase (24-48 hpf) (E) showed increased mitfa expression in tail dorsal stripe melanocytes compared to DMSO-treated embryos (D). In contrast, mitfa mutant embryos treated with BIO throughout the late melanocyte differentiation phase (48-72 hpf) (G) did not show increased mitfa expression compared to DMSO-treated embryos (F) at 72 hpf. 40 zebrafish embryos were investigated for each condition; BIO-treated and matched control embryos were processed for in situ hybridisation in parallel and under identical conditions. H) Quantitation of mitfa expression by RT-qPCR showing significantly increased levels in BIO-treated embryos at 30 hpf compared with untreated controls but not at 48 hpf nor at 72 hpf; data are expressed as percentage of mock-treated controls (control mitfa level = 100 % transcripts (red line on graph)). Gene expression was investigated in triplicate, after normalisation to the stable expression of a reference house-keeping gene, gapdh. Only 15-30 hpf treatment caused significant increase of mitfa expression (t-test, two- tailed: 15-30 hpf, 160.39±7.27 (p=0.0020); 24-48 hpf, 108.15±7.9 (p= 0.0675); 24-72 hpf, 104.6±8.36 (p= 0.544); 24-72 hpf, 86.14±8.96 (p = 0.0831). **, p-value<0.01). I) The effect of the three BIO-treatments applied in the 24-48, 48-72 and 24-72 hpf time windows is shown on Mitfa only as compared to the case of no treatment. The 24-48 and 48-72 hpf BIO-treatments induce an approximately equal increase of Mitfa as measured at the end of the treatment. J) Revised GRN model. Scale bars: 100 µm

205x96mm (300 x 300 DPI)

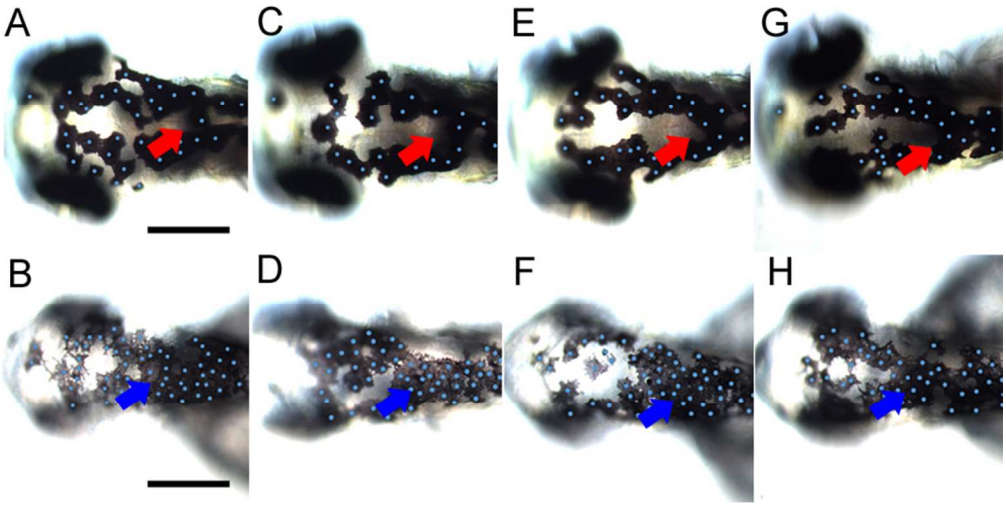

Figure 5: Inactivation of Wnt signalling during melanocyte differentiation enhances melanocyte clustering in posterior dorsal head. Tg(hsp70l:tcf3-deltaC-GFP) embryos were heat shocked at 29 hpf, 36 hpf, 48 hpf and 62 hpf and observed at 73 hpf (B, D, F, H) and compared to control non-heat-shocked transgenic Tg(hsp70l:tcf3-deltaC-GFP) (A, C, E, G). Note the enhanced clustering of melanocytes in the posterior part of the dorsal head in treated embryos (blue arrows) ; the normal distribution in this area in untreated controls is indicated by red arrows. Heat shock activation of Wnt inhibition consistently resulted in smaller heads and eyes. Scale bars: 100 µm.

Unable to Convert Image

The dimensions of this image (in pixels) are too large to be converted. For this image to convert, the total number of pixels (height x width) must be less than 40,000,000 (40 megapixels).

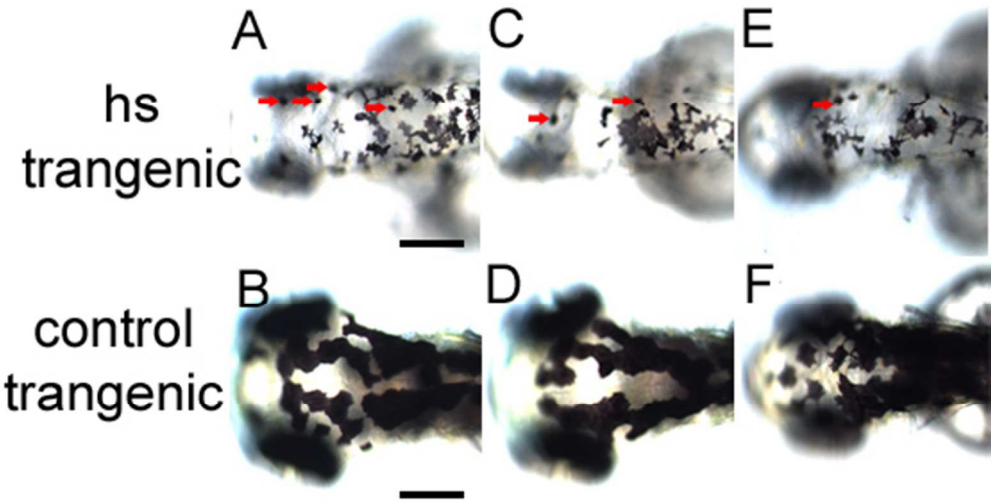

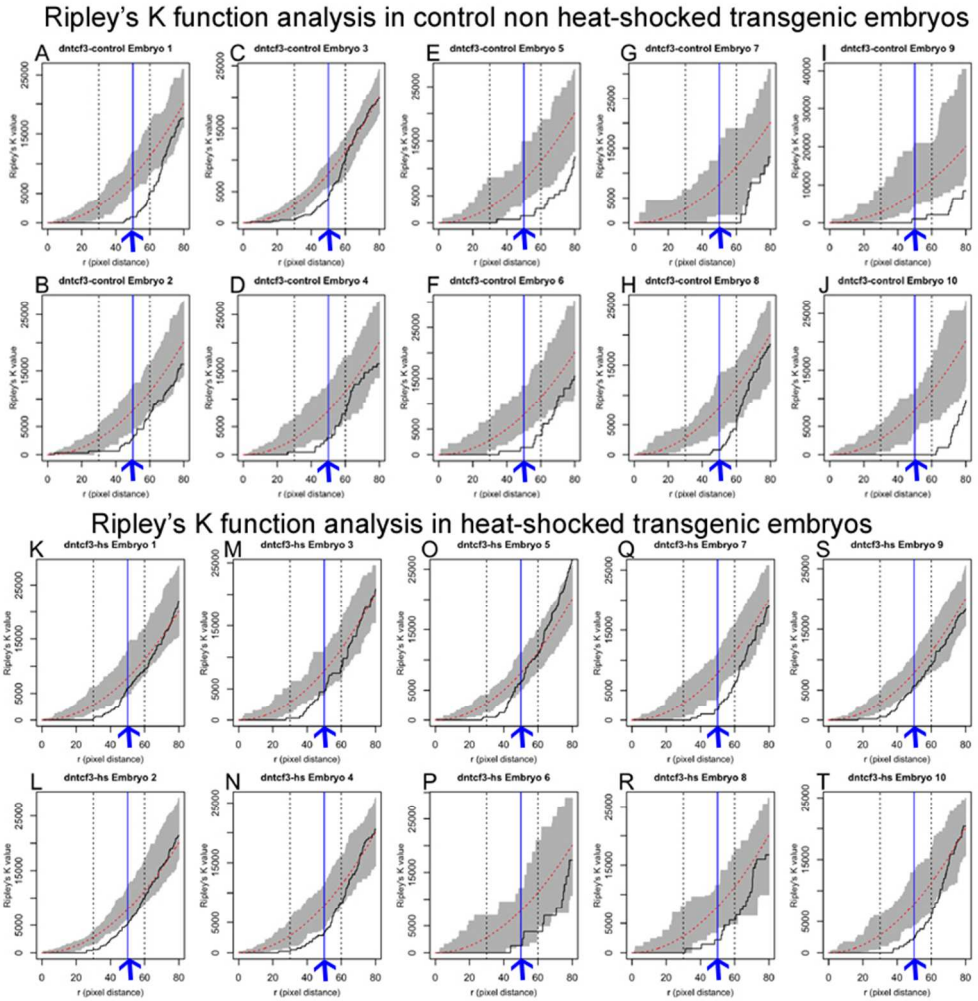
Ripley's K function analysis in control non heat-shocked transgenic embryos
A dntcf3-control Embryo 1
C dntcf3-control Embryo 3
E dntcf3-control Embryo 5
G dntcf3-control Embryo 7
I dntcf3-control Embryo 9
B dntcf3-control Embryo 2
D dntcf3-control Embryo 4
F dntcf3-control Embryo 6
H dntcf3-control Embryo 8
J dntcf3-control Embryo 10
Ripley's K function analysis in heat-shocked transgenic embryos
K dntcf3-hs Embryo 1
M dntcf3-hs Embryo 3
O dntcf3-hs Embryo 5
Q dntcf3-hs Embryo 7
S dntcf3-hs Embryo 9
L dntcf3-hs Embryo 2
N dntcf3-hs Embryo 4
P dntcf3-hs Embryo 6
R dntcf3-hs Embryo 8
T dntcf3-hs Embryo 10
Ripley's K value
r (pixel distance)

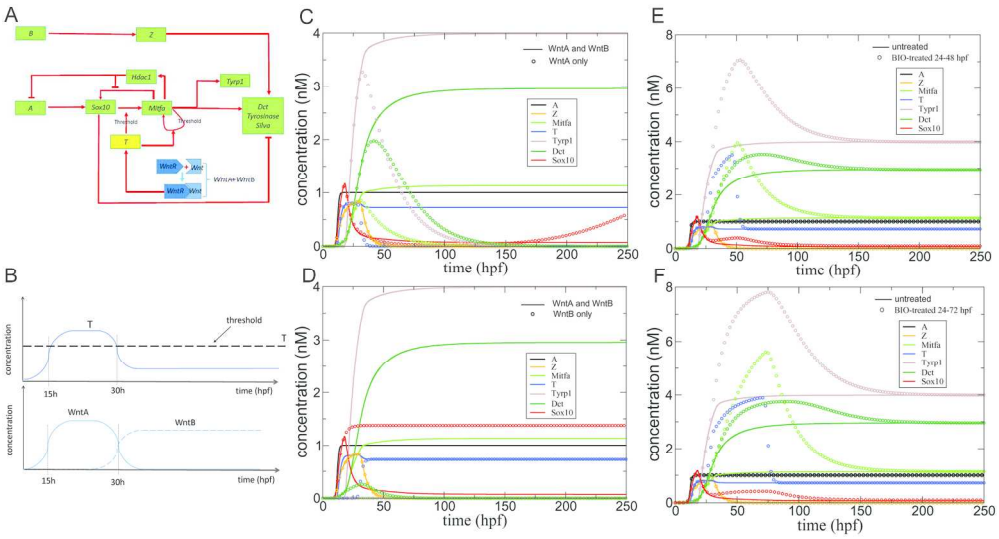

250x137mm (300 x 300 DPI)

An ongoing role for *Wnt* signaling in differentiating melanocytes *in vivo*.

Laura Vibert[1], Gerardo Aquino[2], Ines Gehring[3], Tatiana Subkhankulova[1], Thomas F. Schilling[3], Andrea Rocco[2] and Robert N. Kelsh[1]

Correspondence: Robert Kelsh email: bssrnk@bath.ac.uk

[1]*Developmental Biology Programme, Department of Biology and Biochemistry and Centre for Regenerative Medicine, Claverton Down, University of Bath, Bath, BA2 7AY, UK*
[2]*Department of Microbial and Cellular Sciences, Faculty of Health and Medical Sciences, University of Surrey, Guildford, GU2 7XH, UK*
[3]*Developmental and Cell Biology School of Biological Sciences, University of California, Irvine, 4109, Natural Sciences II, Irvine, CA 92697-2300, USA*

Total word count: 8878

Key words: *Wnt* signaling/ melanocyte/ specification/ differentiation/ zebrafish/ neural crest/ *mitfa*

Running title: Wnt signaling in differentiating melanocytes

Summary

A role for Wnt signaling in melanocyte specification from neural crest is conserved across vertebrates, but possible ongoing roles in melanocyte differentiation have received little attention. Using a systems biology approach to investigate the gene regulatory network underlying stable melanocyte differentiation in zebrafish highlighted a requirement for a positive feedback loop involving the melanocyte master regulator Mitfa. Here we test the hypothesis that Wnt signaling contributes to that positive feedback. We show firstly that Wnt signaling remains active in differentiating melanocytes and secondly that enhanced Wnt signaling drives elevated transcription of *mitfa*. We show that chemical activation of the Wnt signaling pathway at early stages of melanocyte development enhances melanocyte specification as expected, but importantly that at later (differentiation) stages it results in altered melanocyte morphology, although melanisation is not obviously affected. Downregulation of Wnt signaling also results in altered melanocyte morphology and organisation. We conclude that Wnt signaling plays a role in regulating ongoing aspects of melanocyte differentiation in zebrafish.

Significance

Gene regulatory networks underlie all aspects of the development of specific cell-types. While fate specification mechanisms and key genes associated with differentiation are often well-studied, mechanisms leading to maintenance of the differentiated state are less well understood, yet they are crucial from a disease perspective. Positive feedback loops are predicted to be crucial to these maintenance mechanisms. We predicted that such a feedback loop acting on *mitfa* would be crucial for melanocyte maintenance, and provided evidence supporting this hypothesis. Here we provide evidence for the first time that in zebrafish ongoing Wnt signaling is likely to contribute to this feedback loop.

Introduction

Melanocytes are a key derivative of the neural crest, and the mechanisms of melanocyte development are of major interest from developmental and stem cell biology and applied biology perspectives, with clear relevance to understanding human pigmentary disease (Yamaguchi and Hearing 2014; White et al., 2011; Speeckaert et al., 2014; Aoude et al., 2015; Mort et al., 2015). Melanocyte specification from neural crest cells has been relatively well-studied, and has illuminated the underlying mechanisms of neurocristopathies like the Waardenburg syndromes (Dutton et al., 2001; Lee et al., 2000; Southard-Smith et al., 1998; Elworthy et al., 2003). Numerous genes contributing to the differentiated melanocyte phenotype have been described, but little is known of how *stable*

melanocyte differentiation is maintained, although this is likely to be significant in understanding melanoma where reversion to a more progenitor-like state helps drive proliferation and invasiveness (White et al., 2011; Kaufmann et al., 2016). Stability of differentiation is likely to be an emergent property of the state of the gene regulatory network (GRN) in differentiated melanocytes.

Studies in both mouse and zebrafish have shown that melanocyte specification depends upon the expression in neural crest cells of *Microphthalmia-related Transcription Factor (Mitf; mitfa* in zebrafish), which encodes a basic Helix-Loop-Helix transcription factor (Steingrimsson et al., 1994; Hodgkinson et al., 1993; Lister et al., 1999; Watanabe et al., 2002; Opdecamp et al., 1997). *Mitf/mitfa* functions as the master regulator of melanocyte development as it controls all aspects of melanocyte cell biology including melanocyte survival, proliferation, morphology and melanogenesis itself (Steingrimsson et al., 2004; Cheli et al., 2010; Levy et al., 2006; Lister et al., 1999). Transcriptional activation of *Mitf/mitfa* depends upon Sox10, a transcription factor of the Sry-related HMG domain type, shown to bind directly to the *Mitf/mitfa* promoter (Hou et al., 2006; Kelsh 2006; Herbarth et al., 1998; Southard-Smith et al., 1998; Dutton et al., 2001; Elworthy et al., 2003). In addition, Wnt signaling, acting via Lef-1 and β-catenin mediated regulation of *Mitf/mitfa* transcription, is also required for melanocyte specification (Dorsky et al., 1998; Jin et al., 2001; Dorsky et al., 2000; Takeda et al., 2000; Dunn et al., 2000; Lee et al., 2004; Hari et al., 2012). Thus, the combined actions of early Wnt signaling and Sox10 drive expression of Mitf/Mitfa, which acts as a central node in the melanocyte GRN, activating numerous genes associated with all aspects of melanocyte differentiation (Cheli et al., 2010). Importantly, work in zebrafish has shown that a majority of neural crest cells express *mitfa* transiently, but only a subset form melanocytes (Curran et al., 2010). Thus maintenance of *mitfa* expression in a subset of neural crest cells is an important, but under-appreciated, aspect of melanocyte development and, indeed, likely represents a crucial part of the molecular basis for melanocyte fate commitment; cells in which *mitfa* expression is not maintained adopt alternative neural crest fates.

As a first step in understanding how this GRN results in stable maintenance of melanocyte differentiation, we used a systems biology approach, taking advantage of the zebrafish model to allow rapid iterative cycles of mathematical modelling and biological testing of a core melanocyte GRN (Greenhill et al., 2011). Three cycles of this approach resulted in an expanded core network that incorporated a number of hypothetical components for which we also provided experimental support (Fig. 1A; Greenhill et al., 2011). One of these hypothetical components was a predicted Factor Y that enabled stabilisation of melanocyte differentiation by contributing to a positive feedback loop regulating *mitfa* expression (Greenhill et al., 2011). We showed that whilst initial expression of *mitfa* is driven by Sox10, *sox10* then was gradually lost from differentiating melanocytes, being undetectable by *in situ* hybridisation or whole-mount immunofluorescence by c. 50 hours post

fertilisation (hpf). Importantly, we showed that continuing *sox10* expression is not required for melanocyte differentiation and indeed, may even delay this process. In the Greenhill study we showed that Mitfa itself contributed to maintenance of *mitfa* expression, but left the identity of other possible components of the feedback loop unknown.

The canonical Wnt pathway functions via regulation of nuclear β-catenin levels; Wnt protein binding to its transmembrane receptor, Frizzled, displaces glycogen synthase kinase-3β (GSK3β) from the destruction complex, preventing degradation of β-catenin in the cytoplasm, and resulting in elevated β-catenin levels in the nucleus where it functions as a transcriptional activator in co-operation with a co-activator, Lef-1 (Kofahl and Wolf, 2010, Barker, 2008). Canonical Wnt signaling drives fate specification of melanocytes via Tcf/Lef binding to *mitfa* regulatory elements (Dorsky et al., 1998; Dorsky et al., 2000; Takeda et al., 2000; Jin et al., 2001; Hari et al., 2012; Dunn et al., 2000; Lee et al., 2004) although the relevant Frizzled receptor remains elusive (Nikaido et al., 2013). In melanocyte fate specification, Wnt signaling functions in conjunction with Sox10 to drive *mitfa* expression; in a *sox10* mutant, *mitfa* expression is not detectable and melanocytes do not form (Dutton et al., 2001), suggesting that Wnt signaling alone is insufficient to drive *mitfa* expression.

Here we explore two possible modes by which Wnt signaling may also contribute to melanocyte maintenance: 1) by ongoing action alongside Sox10, and 2) in an Mitfa-dependent manner as a component of Factor Y (Figure 1A). We use a transgenic reporter line to show that Wnt signaling is active in melanocytes throughout both specification and differentiation phases. We then use small molecule stimulation of Wnt signaling showing first that it activates *mitfa* expression and is rate-limiting for melanocyte fate specification. We then use this approach to show that stimulating Wnt signaling during melanocyte differentiation affects melanocyte morphology and arrangement according to the timing of treatment. These shape changes correlate with upregulation of *mitfa* expression levels in melanocytes. These *mitfa* expression changes are independent of Mitfa activity in the specification and early differentiation phases, but depend upon Mitfa activity during late differentiation. Conversely, using a transgenic repressor of Wnt signaling, we show that inhibition of Wnt signaling during melanocyte differentiation stages also results in melanocyte shape changes. This is consistent with our proposal that Wnt signaling contributes to an Mitfa-dependent positive feedback loop that maintains melanocyte differentiation, in a manner consistent with our mathematical model of the core melanocyte GRN.

Results

Firstly we asked whether Wnt signaling was active in melanocytes during differentiation. We examined embryos carrying the *Tg(top:GFP)* reporter in which expression of a destabilised GFP

(dGFP) is driven by a promoter containing four consensus LEF1 responsive elements (Dorsky et al., 2002; van de Wetering et al., 1997; Korinek et al., 1997; Dorsky et al., 1998). We scored a sample of melanocytes from these fish throughout melanocyte differentiation (30-72 hpf), using a combination of immunofluorescent detection of dGFP and a low dose of PTU to partially inhibit melanisation to increase sensitivity. We readily detected the activation of dGFP in the tectum as previously described (Figure 1I; Dorsky et al., 2002). We also observed, for the first time, dGFP expression in melanocytes throughout the time-period examined (Figure 1B-G). At early stages the majority of melanocytes (78.5 %) had readily detectable dGFP expression, indicating that most cells at this stage were responding to a Wnt signal. At later stages, a significant proportion of cells still showed detectable dGFP expression, although by 72 hpf the proportion of cells was substantially lower (9 %), but this is likely to at least partly reflect the difficulties of detection of weak fluorescence in even partially-melanised cells.

Having shown that Wnt signaling remains active in melanocytes throughout their differentiation, we then tested the hypothesis that this Wnt signaling in melanocytes might contribute to regulation of their differentiation. We utilised a well-characterised GSK3β inhibitor, Bromoindirubin-3'-oxime (subsequently referred to as BIO), that has been used to investigate the effects of increased Wnt signaling in many model systems, including mammalian cardiomyocyte cell culture, melanoma cells (B16-F0), normal human melanocyte (NHM) cells, mouse embryonic stem cells, and zebrafish (Moro et al., 2012; Alexander et al., 2014; Bellei et al., 2010; Sineva and Pospelov, 2010; Kim et al., 2010; Bellei et al., 2008; Tseng et al., 2006). Consistent with its activation of Wnt signaling in our treated embryos, BIO treatment throughout a 15-40 hpf time-window activated dGFP reporter expression in *Tg(top:GFP)* fish, both in the tectum and in the melanocytes (Figure 1K-L); importantly, this BIO-treatment did not result in gross alterations to embryonic morphology.

Wnt signaling has been shown to drive melanocyte specification from the neural crest in both mouse and zebrafish (Dorsky et al., 1998; Hari et al., 2012). As a further positive control for the efficacy of BIO-treatment in modifying Wnt signaling in our fish, we tested the prediction that BIO treatment in the correct time window would increase melanocyte specification, resulting in elevated melanocyte numbers. We used a shorter treatment phase, focused on 15-30 hpf (Figure 2A), the time when melanocyte specification is thought to occur in the head and trunk. As expected, this treatment resulted in significantly increased melanocyte number in the head of treated embryos compared with controls (Figure 2B-E). Taking advantage of the developmental gradient in these embryos, we examined the trunk and tail region of embryos fixed at the same stage to examine whether elevated melanocyte numbers might be preceded by elevated *mitfa* expression in melanocyte progenitors (premigratory neural crest cells). Consistent with our current working model of the melanocyte GRN, BIO-treated embryos showed increased *mitfa* expression in premigratory neural crest cells compared

with mock-treated controls (Figure 2G-J). Our data suggest that the increased *mitfa* reflects increases in both the levels of *mitfa* expression within a cell and the number of *mitfa*-expressing cells (Figure 2D,E; compare with B,C), consistent with the predicted increase in melanocyte fate specification. Taken together our data support the conclusion that BIO treatment in a 15-30 hpf time-window results in elevated melanocyte specification through increased *mitfa* expression after activation of Wnt signaling. In addition, BIO-treated embryos show a reduction in ventrally-positioned *mitfa*+ cells, suggesting a transient inhibition of melanoblast migration.

Having validated BIO-treatment as an effective method for elevating Wnt signaling, we then addressed our hypothesis that ongoing Wnt signaling might be important for melanocyte differentiation and maintenance. In this study, we divided melanocyte differentiation into early and late phases according to *sox10* expression (Figure 3A). In the early differentiation phase (24-48 hpf) *sox10* expression in melanocytes is decreasing but still detectable by WISH and immunofluorescence, whereas in the late differentiation phase (48-72 hpf), *sox10* is not detectable by WISH or immunofluorescence (Greenhill et al., 2011). We analysed the consequences of boosting Wnt signaling via BIO treatment throughout the entire differentiation phase (24-72 hpf) and during each of the early and late phases of differentiation. Firstly, we tested whether these treatments gave any effects in terms of melanocyte cell number, focusing on the head region. In contrast to 15-30 hpf treatment, no increase in melanocyte number was observed after BIO treatment from 24-48 hpf (control, mean± s.d = 23.9±2.01; BIO, mean±s.d = 23.1±4.03, p=0.443), suggesting that Wnt-dependent melanocyte fate specification is complete in the head region by 24 hpf.

Next we assessed melanocyte differentiation, looking for any changes associated with BIO-treatment during the differentiation phases. In these BIO-treatments, we saw distinctive morphological changes to melanocytes, but interestingly the phenotype differed depending upon the period of BIO treatment. Embryos treated during the early differentiation time window and examined at 48 hpf displayed a dramatic increase in cell dendricity (Figure 3C,E) compared with mock-treated controls (Figure 3B,D). To quantitate this striking phenotype, we used Image J software to estimate the roundness parameter, an established formula relating cell perimeter and cell area (Figure 3F). We found BIO-treatment resulted in a significant increase in cell dendricity compared with mock-treated controls (mean±s.d: control, 2.44± 0.43; BIO, 4.25± 1.68, p = 0.004 (unpaired, one-tailed t-test)). Importantly, this change in cell shape at 72 hpf was not observed in 24-72 hpf (Figure 3G-N) or 48-72 hpf treatments (data not shown) suggesting that this aspect of cell differentiation was only sensitive to Wnt signaling for a period between 24 and 48 hpf, and that the shape changes were only transient. Indeed, where embryos treated in this way were examined at both 48 hpf and 72 hpf, we saw a clear dendricity phenotype at 48 hpf, but this had recovered by 72 hpf (data not shown). In contrast,

embryos treated with BIO from 24-72 hpf showed disorganised melanocytes in the dorsal head; cells were more dispersed, disrupting the 'U' or 'O'-shaped organisation typical of control embryos (Figure 3G-J). Treatment during the late differentiation phase alone (i.e. from 48-72 hpf) resulted in a similar phenotype (data not shown). A Multi-Distance Spatial Cluster Analysis using Ripley's K-Function (Ripley, B.D., 1977) was performed using spatstat package in R (Baddeley & Turner 2005) to quantify the decrease in patterned organisation of melanocytes in the dorsal head using comparable pictures of DMSO and BIO treated fish (Supp. Fig.1). We found that the Ripley's K function confirms the non-random organisation of melanocytes in dorsal heads of DMSO treated embryos (scale of analysis of r=35 pixels). Indeed, at this scale of analysis, for eight of the ten embryos the observed K value was smaller than the expected K value if cells were randomly spread (Supp.Fig.1, A,B,C,E,G,H,J). The result of the Ripley's K analysis performed on BIO treated embryos showed that, at r=35, the observed K values were found within the lower confidence envelop (in the grey area) of the graph meaning that cells were randomly spread in 90% of the cases in nine out of ten embryos (Supp.Fig1K-T). Conversely, 80% of the DMSO population shows a non-random cell organisation and 10% of the BIO treated population shows a non-random cell organisation. A Z-test was then performed to compare the two populations for cellular spatial organisation using the results of this analysis (at r=35, comparing « random » or « not-random »); the two populations were significantly different for this parameter (p-value =0.00164, $p < 0.01$). We conclude that treating embryos with BIO in the early phase of differentiation led to changes in cell shape, whereas ongoing BIO-treatment resulted in changed melanocyte arrangement.

Our working model of the melanocyte GRN predicted that *mitfa* transcription would be increased in response to activation of Wnt signaling. Using quantitative RT-qPCR, we saw a BIO-dependent increase in *mitfa* transcript levels after each of the treatment windows (Figure 4A). *mitfa* expression was increased by around five fold in embryos treated from both 24-48 hpf and 48-72 hpf whereas a nine-fold increase was observed in embryos treated from 24-72 hpf. Combining these data with the melanocyte phenotype changes observed above, we suggest that elevated *mitfa* expression can have distinct effects depending upon whether cells are in a plastic progenitor state (fate specification phase) or are committed to the melanocyte fate (differentiation phase).

Our model (Figure 1A) proposes two modes for Wnt action, one in conjunction with Sox10 and thus unlikely to be significant beyond 48 hpf when *sox10* expression in melanocytes is lost (Greenhill et al., 2011), and one as Factor Y, where it would function as part of a positive-feedback loop with Mitfa, and thus would be dependent upon active Mitfa. To test whether the increase in *mitfa* expression observed in BIO-treated embryos was 1) specific for melanocytes and 2) Mitfa-dependent, we used whole mount in situ hybridisation and RT-qPCR to assess *mitfa* expression in BIO treated *mitfa*^{w2} mutants (Figure 4B-H). The *mitfa*^{w2} mutant is a functional null allele, but expression of *mitfa*

transcripts can be assessed by in situ hybridisation (Johnson et al., 2010). In all cases, *mitfa* expression was restricted to cells with the morphology and distribution consistent with them being neural crest or melanocyte lineage cells, consistent with a cell-autonomous response. Importantly, BIO-treatment of *mitfa*^{w2} mutants in a 15-30 hpf window (i.e. during cell specification, when *sox10* is relatively strongly expressed in the melanocyte lineage) resulted in increased *mitfa* expression (Figure 4H), most clearly seen as increased numbers of cells expressing relatively high levels of *mitfa*, at 30 hpf compared with mock-treated embryos (Figure 4B,C). A 24-48 hpf BIO-treatment, assessed at 48 hpf, showed an elevated level of *mitfa* expression in *mitfa*^{w2} mutants, at least in the dorsal tail (Figure 4D,E). In contrast, BIO-treatment in a 24-72 (data not shown) or 48-72 hpf window (Figure 4F,G), assessed at 72 hpf, did not show elevated *mitfa* transcription in these *mitfa*^{w2} mutants (Figure 4H), suggesting that the Wnt-mediated effect is Mitfa-dependent. Quantitation of *mitfa* expression levels using RT-qPCR confirmed the significant increase in *mitfa* expression after 15-30 hpf treatment even in *mitfa*^{w2} mutants, and the absence of a significant response after the 24-72 and 48-72 hpf time-windows. Our quantitative assay did not detect the change after a 24-48 hpf time-window: although consistently detectable by the semi-quantitative whole-mount in situ hybridisation technique, which has the advantage of assessing individual cells in different spatial domains, this signal is apparently masked by the general signal coming from the head and trunk. We conclude that Wnt inputs on *mitfa* expression act initially through the Sox10-dependent mechanism, but then switch to functioning through a Sox10-independent, Mitfa-dependent positive feedback loop.

As a complement to these gain-of-function studies, we tested the effects of loss of Wnt signaling activity during melanocyte differentiation using a conditional activation of the dominant negative T-cell Factor 3 (Tcf3) in transgenic zebrafish carrying *Tg(hsp70l:tcf3-deltaC-GFP)* (Martin and Kimelman, 2012). As before, we tested the functionality of our experimental system by inducing heat-shock during the specification phase of melanocyte development, from 15 to 28 hpf, and assessing first activation of GFP fluorescence and expression of Wnt signaling targets such as *mitfa*, by RT-qPCR. Both activation of GFP and downregulation of *mitfa* expression were observed after heat-shock (data not shown). To assess the requirement for ongoing Wnt signaling in melanocyte differentiation, we heat-shocked embryos at each of four timepoints, 29 hpf, 36 hpf, 48 hpf, and 62 hpf before assessing melanocyte phenotypes in the dorsal head at 73 hpf. Two populations of embryos could be distinguished by the level of activation of GFP, one where embryos showed strong GFP fluorescence and the second population showing weak GFP fluorescence; we note that in almost all cases melanocytes were abundant, indicating that survival of melanocytes was usually not affected, although in a subset of the fish exhibiting strong GFP, melanocyte number was visibly reduced. In the first population (strong inhibition of Wnt signaling) melanocyte melanisation, apparent morphology and patterning were all abnormal, but since the gross anatomy of the embryos was also affected, these melanocyte phenotypes were not quantitated. However, we noticed that a subset of melanocytes in

each fish was abnormally rounded, melanisation was always reduced and these cells were abnormally patterned (Supp. Fig. 2). In the second population (weak inhibition of Wnt signaling), melanocyte morphology was more normal, but their patterning was modified compared to non heat-schocked siblings (Figure 5). We observed enhanced clustering of melanocytes, particularly in the posterior region of the dorsal head (Figure 5B,D,F,H, blue arrow). Again, we used Multi-Distance Spatial Cluster Analysis using Ripley's K-Function (Ripley, B.D. (1977)) to quantify the change in patterned organisation of melanocytes in the dorsal head using comparable pictures (Supp. Fig. 3). This analysis showed that whereas 90% of the non-heat-shocked *Tg(hsp70l:tcf3-deltaC-GFP)* embryos showed "non-random" pattern, 70 % of the heat-shocked *Tg(hsp70l:tcf3-deltaC-GFP)* embryos showed loss of organisation (« random » cell organisation – the combination of the clustered melanocytes in the posterior head and the unclustered melanocytes in the anterior head are together scored by the algorithm as more randomly organised using this scale of analysis)(scale of analysis of r=50 pixels). A Z-test comparing the two populations for cellular spatial organisation using the results of this analysis (at r=50, comparing « random » or « not-random ») showed they were significantly different for this parameter (p-value = 0.00244, $p < 0.01$). We conclude that inactivating Wnt signaling during melanocyte differentiation in *Tg(hsp70l:tcf3-deltaC-GFP)* using heat shock led to significantly increased clustering of melanocytes in the posterior part of the dorsal head. We note that this loss-of-function phenotype is complementary to the gain-of-function phenotype using drug treatment, suggesting that Wnt signaling has a consistent impact on melanocyte differentiation in zebrafish *in vivo*.

We used the mathematical modelling approach we developed before (Greenhill et al., 2011) to assess the effects of including Wnt signaling (Supp. Fig. 3A). We incorporated Wnt signaling in both fate specification and differentiation phases by assuming Wnt expression to activate β-catenin/Lef-1 (abbreviated as T), coupled in turn with an AND gate to Sox10 during specification, and by another AND gate to Mitfa during commitment. For such a highly migratory cell-type, melanocyte fate specification (in/near the dorsal neural tube) and melanocyte differentiation (during dispersion and in post-migratory locations) are usually anatomically distinct and, given the complexity of Wnt expression patterns, thus are intuitively likely to involve distinct Wnt family members. Thus, we postulated two independent Wnt signals, one (WntA) acting in an early, but transient, time window lasting to approximately 30 hpf, and another (WntB) beginning at that latter time point and extending throughout differentiation. We also assumed a threshold level of T required to trigger a response from the AND gate between Sox10 and T (Supp. Fig.3A,B), and a threshold level of Mitfa to avoid accidental activation of the Mitfa feedback loop (see Greenhill et al., 2011). As in Greenhill et al. (2011) one of the key outcomes used to judge the appropriateness of the subsequent simulations was that *mitfa* expression initially rose, and then was maintained at a substantial level. Indeed, under normal conditions our revised model results in expression profiles comparable to those of the original

Greenhill Model C (Greenhill et al., 2011). Moreover, modelling the effects of mutating the two Wnt signals independently behave as expected intuitively (Supp. Fig. 3C,D). In particular, in the absence of the first Wnt signal, WntA, melanocyte specification fails and *mitfa* expression remains absent (Supp. Fig. 3C); likewise, in the absence of the second Wnt signal, WntB, *mitfa* expression peaks transiently before disappearing rapidly, so that maintenance of the differentiated state fails (Supp. Fig. 3D). Currently, Wnt8 has been proposed as an inducer of neural crest in zebrafish (Lewis et al., 2004), but knowledge of the Wnt signals underlying melanocyte development in fish is very limited, although Wnt8 has been shown not to be critical (Dorsky et al., 1998; Lewis et al., 2004); a testable prediction of our modelling is that two distinct Wnt signals drive early melanocyte fate specification versus later maintenance of differentiation.

We then assessed *in silico* the effect of increasing Wnt signaling strength in each of the specification and (early, late and full) differentiation phases. We did this by modifying the amount of WntA and WntB driving expression of T, and simulating accordingly the GRN response. We modelled the derepression of the Wnt signal due to the action of the BIO-treatment as a linear increase in time of WntA/B. As a consequence we expected the elevated expression of *mitfa* induced by BIO to be proportional to the duration of the BIO-treatment. Indeed, by choosing parameter values compatible with values in the literature (see Materials and Methods), the simulations show a relative increase of Mitfa expression in response to BIO compatible with the experimental data (Fig. I). In particular we show that when BIO is applied for the same amount of time (namely in the time windows 24-48hpf and 48-72hpf) the increase in *mitfa* is approximately the same. In contrast, when BIO is applied between 24-72 hpf, our simulations show a larger *mitfa* increase, roughly comparable with the observed linear dependency. Thus, our revised model with its more precise delineation of the roles of Wnt signals at different phases in melanocyte development continues to correspond well to the key experimental observations *in vivo*.

Our observation that elevated Wnt signaling in the specification phase results in more cells becoming melanocytes is readily accounted for by the model through the threshold on T. The likelihood of an *mitfa*-expressing cell maintaining *mitfa* expression and thus differentiating into a melanocyte depends on T being above this threshold in the specification phase. In a population of cells, we expect stochastic variations in the levels of WntA (and hence T) will result in this condition not being satisfied in some cells. If BIO is applied early, T levels are enhanced, and therefore during the specification phase (i.e. prior to commitment) the proportion of cells proceeding successfully towards the melanocyte state is predicted to increase. In contrast, if BIO is only applied later, T levels during the earlier specification window are unaffected, so no change in the final number of melanocytes is predicted, in agreement with our experimental data.

Discussion

We conclude that in addition to the established role for Wnt signaling in melanocyte specification from the neural crest, Wnt signaling has an ongoing influence on melanocyte differentiation at least until 72 hpf. By using a transgenic reporter strain we demonstrated that Wnt signaling remained detectable in differentiated melanocytes until 72 hpf at least. We then used BIO to assess the effects of increased Wnt signaling on melanocyte development in zebrafish embryos, showing that such treatment resulted in elevated *mitfa* expression in the neural crest and melanocyte lineage cells. Interestingly, we observed defects in melanocyte morphology with an increase in cell dendricity at 48 hour post fertilisation (hpf) and altered cell organisation at 72 hpf. We complemented these gain-of-function studies with a loss-of-function approach, using a conditional dominant negative transgenic line to inhibit Wnt signaling activity during melanocyte differentiation phases. Importantly, our data showed that this resulted changes in melanocyte morphology (when dnTcf3 strongly expressed), resulting for example in enhanced clustering of melanocytes in the posterior head. This study demonstrates for the first time a function for Wnt signaling in zebrafish melanocytes, beyond the well-known role in melanocyte fate specification, showing that it is important for multiple aspects of melanocyte differentiation. We note that our data indicates that the mode of Wnt signaling input changes from an Mitfa-independent/Sox10-dependent early role to an Mitfa-dependent/Sox10-independent later role, suggesting that Wnt signaling at late stages becomes incorporated into the melanocyte maintenance (Factor Y) role postulated in our earlier work. We have revised our working model of the core GRN of melanocyte development in zebrafish to incorporate these new data (Figure 4J). It is likely that Wnt signaling has a similar role in mammalian melanocytes since GSK3β inhibition results in upregulation of *MITF* expression and differentiation in normal human melanocytes, at least in cell culture (Bellei et al., 2008).

Although we show here that Wnt signaling continues to influence melanocyte differentiation, our gain-of-function experiments do not cause obvious effects on melanisation. However, we note that our modelling data (Supp. Fig. 3E,F) indicates that this may be quantitatively relatively subtle (e.g. for *dct* in curves shown), so our failure to detect such an effect in vivo may be simply due to lack of sensitivity in our assay. A study of normal human melanocytes in tissue culture showed that GSK3β inhibition stimulated melanogenesis through activation of *MITF* (Bellei et al., 2008). In contrast, in our loss-of-function experiments, those embryos showing highest levels of GFP and in which Wnt signaling was presumably most inhibited, showed a pronounced reduction in both melanin levels and defects in apparent cell morphology. Thus, it seems that Wnt signaling is important for all aspects of melanocyte differentiation, consistent with its effects on expression of *mitfa*.

The role for Wnt/β-catenin signaling in melanocyte specification through induction of *Mitf* expression is conserved in fish and mammals (Dorsky et al., 2000; Takeda et al., 2000). Our work showing that inhibition of GSK3-β using BIO stimulates melanoblast specification (*mitfa* expression) adds further support to this conclusion. Importantly, no increase in melanocyte cell number in the dorsal head was observed after 24-72 hpf treatments suggesting that melanocyte specification from neural crest cells does not extend much beyond 24 hpf. Furthermore, our time window studies showed that treatment from 15-30 hpf was sufficient to generate elevated numbers of head melanocytes that persist until at least 72 hpf, whereas treatment in a 24-48 hpf window did not. These data indicate, for the first time to our knowledge, that commitment to the melanocyte fate in zebrafish (at least for melanocytes in the head region that arise in the embryo) has occurred by c. 30 hpf. As explained above, melanocyte specification reflects *maintenance* of *mitfa* expression in NCCs, so our data suggest that this process is limited by Wnt signaling.

Our data demonstrate intriguing Wnt-dependent effects on melanocyte morphology and organisation. An *in vitro* study of normal human epidermal melanocytes demonstrated that increased and decreased levels of active β-catenin resulted in increased and decreased cell dendricity respectively *(*Kim et al., 2010). They further showed that this resulted from activation of distinct downstream modulators, PKCf and PKCd, respectively (Kim et al., 2010). They showed that overexpression of PKCf resulted in the decrease of protein levels for Rac1 and Cdc42 and consequently a reduction of dendrite formation in melanocytes, while overexpression of PKCd led to increase of Rac1 and Cdc42 and an increase in melanocyte dendrites. We show here that elevated Wnt signaling results in increased *mitfa* expression and increased dendricity, suggesting a causal link between *mitfa* expression levels and cell shape. This idea is strongly supported by earlier studies in Xenopus embryos showing that increased *X-mitfa* expression resulted in increased melanocyte dendricity and cell dispersal (Kumasaka et al., 2005; Kawasaki et al., 2008). Further studies will be required to test whether Wnt signaling in zebrafish causes increased melanocyte dendricity through a pathway of *mitfa*-dependent activation of PKCd, elevated levels of activated Rac and Cdc42, and consequent modifications of the actin cytoskeleton.

In summary, our work defines two phases of Wnt signaling involvement in zebrafish melanocyte development *in vivo*, both of which are likely conserved in mammals. Recent analysis showed that the two transcription factors Tfap2a and Tfap2e are required for early melanocyte differentiation, through both maintenance of *kit* expression and another mechanism still to be defined (Van Otterloo et al., 2010). It will be of interest to assess whether these roles for Tfap2 factors extends to ongoing maintenance of the differentiated state and, if so, the extent to which Wnt signaling and Tfap2/Kit function are integrated in this system.

Figure legends

Figure 1.

Ongoing Wnt signaling is detectable in differentiating melanocytes.

(A) Diagram of working model for melanocyte core GRN (modified from Greenhill et al., 2011). Note two inputs from Wnt signaling on *mitfa* expression, one well-established role acting alongside Sox10 driving melanocyte fate specification, and hypothetical role explored here as part of a positive feedback loop also involving Mitfa itself. B-G) Wnt signaling in differentiating melanocytes was assessed by scoring samples of melanocytes for detection of dGFP by immunofluorescence in *Tg*(*top:GFP*) transgenic embryos from 30-72 hpf. GFP-positive melanocytes (arrows) are shown by immunofluorescence (B,D,F) and DIC (C,E,G) to show melanin pigment. At each stage, 30 melanocytes in each of 15 embryos were assessed for GFP expression, in the dorsal head and throughout the dorsal and lateral trunk; numbers show the percentage of melanocytes expressing GFP (mean ± s.d) at corresponding stages (n = 450 per stage). H) Schematic showing timing of BIO treatment used. I-L) BIO-treatment enhances activity of *Tg(top:GFP)* reporter. BIO-treatment from 15 hpf to 40 hpf dramatically enhances dGFP expression (red arrows) in the tectum of treated (K) compared with mock-treated controls (I) and also increases dGFP signal in melanocytes of *Tg(top:GFP)* embryos (BIO-treated (L) compared with mock-treated control (J)). All images, lateral views using confocal microscopy. EM, embryo medium; e: eye; T: tectum. Scale bars: B-G) 10 µm; I-L) 100 µm.

Figure 2.

Elevated Wnt signaling in melanocyte specification time window increased numbers of melanocytes. A) Schematic showing timing of BIO treatment or control mock-treatment (DMSO alone) used. B-E) Lateral views of the trunk of live 30 hpf zebrafish embryos showing melanocytes (red arrows); note increased number in both anterior (D) and posterior trunk (E) of embryos treated with 5 µM BIO compared with control DMSO treated embryos (B,C respectively). F) Quantitation of increased melanocyte number in heads of BIO-treated embryos (mean ± s.d.; control, 13 ± 2.1; BIO, 32 ± 5.3, $p<10^{-6}$) (n= 20; *** indicates significant difference between treated and mock-treated; unpaired, one-tailed t-test). G-J). Lateral views of posterior trunk (G,I) and close-up of anterior tail (H,J) of 30 hpf zebrafish embryo in situ hybridisations to show *mitfa* expression in embryos treated with BIO (I,J) or DMSO control (G,H). In the DMSO control embryos (G,H) discontinuous *mitfa* expression is observed in the dorsal region (blue arrows show discontinuities of the signal), whereas in the BIO treated embryos (I,J) *mitfa* expression is continuous throughout the dorsal region (red arrows). Images show representative phenotypes (n=20 per treatment). Scale bar: 100 µm.

Figure 3: Elevated Wnt signaling in melanocyte differentiation time window alters melanocyte morphology. A) Schematic of melanocyte differentiation BIO-treatment time-windows. B-E)

Activation of Wnt signaling in early differentiation period (24-48 hpf) increases melanocyte dendricity and dispersion. Lateral view at 48 hpf of head of live embryos treated with control DMSO (B) or BIO (C) from 24-48 hpf. Panels D and E show enlargements of head melanocytes from embryos in B and C respectively. F) Quantitation of dendricity: the cell roundness parameter was calculated for each melanocyte as R = P2/4∏A, where A is the cell area and P the cell perimeter, 20 cells were investigated (n=20) in 10 different embryos for each condition. A score of R=1.0 represents a perfectly round melanocyte; increased R values represent increased dendricity. Control, R=2.44 ± 0.43, BIO R= 4.25 ± 1.68, p = 0.004, t-test result, p-value<0.01 (**). G-J) Elevated Wnt signaling throughout full differentiation or during late differentiation window only affects melanocyte organisation. Red line in G indicates the dorsal head melanophores which usually approximate an O- or U-shaped pattern, although often with extra branches as in this specific example. Dorsolateral view at 72 hpf of heads of live embryos treated with control DMSO (G,I,K,M) or BIO (H,J,L,N) from 24-72 hpf shown. Note that embryos treated in only Late Differentiation window (48-72 hpf) show equivalent phenotype (data not shown). Embryos shown are representative of samples examined (n=160 zebrafish embryos for each treatment). Scale bars: 100 µm (B,D,G,I).

Figure 4: Positive feedback between Wnt signaling and Mitfa during late differentiation phase of melanocyte development. A) Quantitation of *mitfa* expression by RT-qPCR showing significantly increased levels in BIO-treated embryos compared with untreated controls; data are expressed as percentage of mock-treated controls (control *mitfa* level = 100 % transcripts (red line on graph)). Gene expression was investigated in 10 samples consisting of the trunk and tail of 50 embryos for each condition and in triplicate, after normalisation to the stable expression of a reference house-keeping gene, *gapdh*. All treatments caused significant increase of *mitfa* expression (t-test, two- tailed: 24-48 hpf, 535±7.1 (p= 0.00087); 48-72 hpf, 496±9.8(p= 0.0085); 24-72 hpf, 872±32.1 (p = 0.000092). ***, p-value<0.001). B-G) Activating Wnt signaling after 48 hpf does not affect *mitfa* expression in *mitfa*^{w2} mutant embryos during melanocyte differentiation. Lateral views of trunk showing in situ hybridisation for *mitfa* expression in *mitfa* mutant fish. *mitfa* mutant embryos treated with BIO in the melanocyte specification phase (15-30 hpf) (C) showed increased *mitfa* expression (purple) compared to DMSO-treated embryos (B). Similarly, *mitfa* mutant embryos treated with BIO in the melanocyte early differentiation phase (24-48 hpf) (E) showed increased *mitfa* expression in tail dorsal stripe melanocytes compared to DMSO-treated embryos (D). In contrast, *mitfa* mutant embryos treated with BIO throughout the late melanocyte differentiation phase (48-72 hpf) (G) did not show increased *mitfa* expression compared to DMSO-treated embryos (F) at 72 hpf. 40 zebrafish embryos were investigated for each condition; BIO-treated and matched control embryos were processed for in situ hybridisation in parallel and under identical conditions. H) Quantitation of *mitfa* expression by RT-qPCR showing significantly increased levels in BIO-treated embryos at 30 hpf compared with untreated controls but not at 48 hpf nor at 72 hpf; data are expressed as percentage of mock-treated

controls (control *mitfa* level = 100 % transcripts (red line on graph)). Gene expression was investigated in triplicate, after normalisation to the stable expression of a reference house-keeping gene, *gapdh*. Only 15-30 hpf treatment caused significant increase of *mitfa* expression (t-test, two-tailed: 15-30 hpf, 160.39±7.27 (p=0.0020); 24-48 hpf, 108.15±7.9 (p= 0.0675); 24-72 hpf, 104.6±8.36 (p= 0.544); 24-72 hpf, 86.14±8.96 (p = 0.0831). **, p-value<0.01). I) The effect of the three BIO-treatments applied in the 24-48, 48-72 and 24-72 hpf time windows is shown on Mitfa only as compared to the case of no treatment. The 24-48 and 48-72 hpf BIO-treatments induce an approximately equal increase of Mitfa as measured at the end of the treatment. J) Revised GRN model. Scale bars: 100 µm

Figure 5: Inactivation of Wnt signalling during melanocyte differentiation enhances melanocyte clustering in posterior dorsal head. *Tg(hsp70l:tcf3-deltaC-GFP)* embryos were heat shocked at 29 hpf, 36 hpf, 48 hpf and 62 hpf and observed at 73 hpf (B, D, F, H) and compared to control non-heat-shocked transgenic *Tg(hsp70l:tcf3-deltaC-GFP)* (A, C, E, G). Note the enhanced clustering of melanocytes in the posterior part of the dorsal head in treated embryos (blue arrows) ; the normal distribution in this area in untreated controls is indicated by red arrows. Heat shock activation of Wnt inhibition consistently resulted in smaller heads and eyes. Scale bars: 100 µm.

Supplemental data

Supplementary Figure 1: Ripley's K function analysis shows significant decrease in melanocyte organisation in BIO-treated embryos compared to DMSO-treated embryos at 72 hpf.
Ripley's K function analysis was performed on 10 DMSO treated embryos (A-J) and 10 BIO treated embryos (K-S). The expected values for K if the cells are randomly spread are represented by the red dotted line on the graph; the grey area corresponds to area between the lower and higher confidence envelope/interval for values of K. Based on inspection of control embryos, and noting that the dorsal head melanocytes are clearly patterned, we set the scale of analysis to r=35 pixels (blue arrows and blue lines). Significant clustering then corresponds to the white zone underneath the grey area whereas significant dispersion corresponds to the white area above the grey area. As expected, 8 out of 10 DMSO-treated control embryos are scored as showing a clustered pattern (below the grey area; embryos A-E,G,H,J). In contrast, Ripley's K function analysis performed on BIO treated embryos showed that the observed K values were found within the lower confidence envelope (in the grey area) of the graph in nine out of ten embryos (embryos K-S), so that cells appeared randomly dispersed in 90% of the cases.

Supplementary Figure 2: Strong expression of a dntcf3 transgene results in poor melanocyte differentiation. Transgenic *Tg(hsp70l:tcf3-deltaC-GFP)* embryos **t**hat were heat shocked at each of 29, 36, 48 and 62 hpf and which showed strong GFP expression (A,C,E) demonstrate a strong melanocyte phenotype including reduced melanisation and more rounded shape (red arrowheads) at 73 hpf compared to non-heat-shocked control transgenic embryos (B,D,F). Scale bars: 100 μm.

Supplemental Figure 3: Ripley's K function analysis shows significant decrease in melanocyte organisation when Wnt signalling is impaired in dntcf3 transgenic embryos at 72 hpf. Ripley's K function analysis was performed on 10 control non-heat-shocked transgenic *Tg(hsp70l:tcf3-deltaC-GFP)* embryos (A-J) and 10 heat-shocked transgenic *Tg(hsp70l:tcf3-deltaC-GFP)* embryos (K-T). The expected values for K if the cells are randomly spread are represented by the red dotted line on the graph; the grey area corresponds to area between the lower and the higher confidence envelope/interval for values of K. Based on inspection of control embryos, and noting that the dorsal head melanocytes are clearly patterned, we set the scale of analysis to r=50 pixels (blue arrows and blue lines). Significant clustering then corresponds to the white zone underneath the grey area whereas significant dispersion corresponds to the white area above the grey area. As expected, eight out of ten control embryos are scored as showing a clustered pattern (below the grey area; embryos A-E,G,H,J). In contrast, Ripley's K function analysis performed on heat-shocked embryos showed that the observed K values were found within the lower confidence envelope (in the grey area) of the graph in seven out of ten embryos (embryos K-S), so that cells showed 'lower organisation' in 70% of the cases.

Supplementary Figure 4:

A) Core GRN for melanocyte differentiation activated by Wnt signaling. Extension of Gene Regulatory Network as from Greenhill et al., (2011) with inclusion of β-catenin/Lef-1 (indicated in the diagram as T) mediated Wnt activation. The complex β-catenin/Lef-1 is assumed to work in conjunction with Sox10 and Mitfa through AND gates. Two components of Wnt signaling (WntA and WntB) are also assumed to participate selectively in fate specification and commitment respectively.

B) Schematic of WntA and WntB signaling.

We show the time profile of the Wnt components, WntA and WntB, as used in this model. The first component is active between times 15-30 hpf and activates production of nuclear T (plotted) above the threshold value while the second component is active for times beyond 30 hpf and has a lower affinity not enough to induce a production of T above threshold. Note that although modelled here as differences in affinity for their receptors, exactly equivalent outcomes would result if their affinities were identical, but WntA and WntB expression levels differed.

C-D) Selective failure of specification and commitment.

We plot the response of the GRN to either Wnt component acting alone. When only WntA is active (C) we have specification but only transient differentiation (Mitfa increases initially, but then decays to zero) while when only WntB is active (D) Mitfa production is never observed. The traces of Sox10 (red curve), Z (orange), T (blue), Dct (dark green), Tyrp1 (brown), A (black) and Mitfa (light green) are plotted as a function of time (hours after fertilisation, hpf).

E-F) Simulation of the core GRN according to the mathematical model (see Methods).
The traces of Sox10 (red curve), Z (orange), T (blue), Dct (dark green), Tyrp1 (brown), A (black) and Mitfa (light green) are plotted as a function of time (hrs). Solid lines correspond to time-courses without BIO treatment while circles correspond to those with BIO treatment. E) BIO treatment is applied between 24 and 48 hpf, Mitfa (light green circles) is amplified 2-fold at 48 hrs as compared to the evolution without BIO treatment (light green line) at the same time. F) BIO treatment is applied between 24 and 72 hpf, Mitfa (light green circles) is amplified 3-fold at 72 hrs as compared to the evolution without BIO treatment (light green line) at the same time.

Methods

Fish Husbandry

Wild type (AB) and transgenic *Tg(-7.2sox10:EGFP*) (Carney et al., 2006) and *Tg(top:GFP))* (Dorsky et al., 2002) and mutant *mitfa*^{w2} (Lister et al., 1999) zebrafish, *Danio rerio*, were kept in the aquarium at the University of Bath. *Tg(hsp70l:tcf3-deltaC-GFP) (*=w26Tg) fish (Martin and Kimelman, 2012) were kept in the facilities of the Department of Developmental and Cell Biology, School of Biological Sciences at the University of California, Irvine. Natural crosses were set up overnight and embryos collected in the morning. Embryos were placed in embryo medium and grown at 28.5 °C. They were staged according to Kimmel et al., (1995). Where embryos were to be manipulated between laying and hatching we used Watchmakers' No5 forceps to dechorionate the embryos. Embryos older than 15 hpf which were to be manipulated in any way were anaesthetised with Tricaine (Ethyl 3-aminobenzoate methanesulphonate, 4 g/L stock, final concentration approximately 0.2 % v/v). Where appropriate, melanisation was inhibited using PTU (1-phenyl-2-thiourea) from 24 hpf at a final concentration of 0.0015 % in embryo medium. All experiments complied with institutional and national animal welfare laws, guidelines and policies. Procedures involving fish older than 5 dpf were undertaken under licence from the UK Home Office.

BIO (2'*Z*,3'*E*)-6-Bromoindirubin-3'-oxime) treatment

BIO (2'*Z*,3'*E*)-6-Bromoindirubin-3'-oxime)*:* GSK3β inhibitor (Calbiochem) was stored as a 10 mM stock solution in DMSO. Ten wild type or *mitfa*^{w2} mutant embryos were placed in triplicate into 6-cm petri dishes containing 8 ml embryo medium. All embryos were dechorionated before 10 mM BIO

(361550 GSK-3 Inhibitor IX, Calbiochem) in DMSO was added to each experimental dish to a final concentration of 5 µM; an equivalent volume of DMSO was added to the control dishes. Embryos were incubated under standard conditions from 15-30, 24-48, 48-72 or 24-72 hpf.

Heat-shock experiment

Tg(hsp70l:tcf3-deltaC-GFP) transgenic embryos (Martin and Kimelman, 2012) were heat shocked at 39°C for 12 minutes at four timepoints (29 hpf, 36 hpf, 48 hpf and 60 hpf) during melanocyte differentiation; after heat-shock, embryos were assessed for GFP expression and left to develop at 28.8°C in incubator. Embryos were assessed for melanocyte differentiation defects at 73 hpf.

Whole mount *in situ* hybridisation

RNA *in situ* hybridisation was performed according to Thisse and Thisse, (2008) except probes were not hydrolysed and embryos were incubated at 68 °C in hybridization steps. Probes used were *sox10* (Dutton et al., 2001), *mitfa* (Lister et al., 1999), *xdh* (Parichy et al., 2000). (Plasmid and probe generated by T. Chipperfield and C. Nelson).

RNA extraction and cDNA synthesis

RNA was extracted from samples consisting of 50 whole embryos of each condition using TRI REAGENT (Sigma-Aldrich, T9424) according to manufacturer's instructions and purified and precipitated by phenol/chloroform/isoamylalcohol (25:24:1). The RNA pellet was washed in 1ml 75% ETOH by inverting the tube gently. A 1 µl sample was assessed for purity, integrity by gel electrophoresis, and concentration was measured spectrophotometrically. When required, samples were stored at -80°C for not more than a month. For experiment using WT embryos, first strand cDNA was synthesised using the Invitrogen First strand cDNA synthesis kit with Superscript III and oligodT (Promega), 0.5 µl random hexamers (250ng/µl) (Promega), 5 µl dNTPs (2mM) (Promega), 7.5 µl RNA (1 µg of total RNA) were first mixed and incubated for 5 mins at 65^{o}C and then at least 1 min at 4^{o}C. Second, 4 µl of 5X first strand buffer (Invitrogen), 1 µl of 5mM DTT, 1 µl RNAse out (Invitrogen) and 1 µl superscript III (Invitrogen) RTase/Mµl were added to the previous mix and left 5 minutes at 25 ^{o}C, 60 ^{o}C minutes at 50 ^{o}C, 15 minutes at 70 ^{o}C. Finally, samples were diluted 1:5 and concentrations were measured spectrophotometrically. For experiments using mitfa^{w2} mutant embryos, RNA extraction was performed by Direct-zol™ RNA MiniPrep (Zymo Research) and the iScript™ Advanced cDNA Synthesis Kit (Bio-Rad) was used for reverse transcription of 1 µg RNA in 20 µl reaction according to manufacturer's protocol.

Real-time quantitative PCR

.Real time quantitative PCR was performed in triplicate using SYBR Green I PCR Master Mix (Roche) for WT embryos and a Lightcycler II machine (Roche) was used according to the manufacturer's instructions. For *mitfa*^{w2} mutant embryos, the Fast SYBR® Green Master Mix (ThermoFisher) was used and samples were run in triplicate using the StepOne™ System (ThermoFisher) according to manufacturer's instructions. Standard curves for both *gapdh* and *mitfa* primers demonstrated nearly 100% efficiency (98.7% and 98.5%, correspondently). Primers were designed spanning an intron using Primer3 Plus software (http://www.bioinformatics.nl/cgibin/primer3plus/primer3plus.cgi.). The following primers were used:

gapdh: forward 5'ACCAACTGCCTGGCTCCT3',
reverse 5'TACTTTGCCTACAGCCTTGG3';

mitfa: forward 5'CTGGACCATGTGGCAAGTTT3',
reverse 5'GAGGTTGTGGTTGTCCTTCT3'

Gene expression was normalized against zebrafish *gapdh* expression in wild-type embryos. RT-qPCR data were analysed using the (ΔΔCt) method (Livak et al., 1998). Student's t-test was performed using GraphPadPrism 5.0. In all tests, difference was considered significant if $p<0.001$.

Immunofluorescence

Embryos for immunofluorescent detection were processed following the protocol proposed by (Ungos et al., 2003). Embryos were fixed in 4 % Paraformaldehyde in PBS (Phosphate buffered saline, Oxoid) overnight at 4 °C. They were washed three times for 5 minutes in PBTriton (0.1 % Triton X-100 Sigma-Aldrich in PBS) and three times for one hour in MilliQ water. Embryos were incubated in block solution (1 % DMSO, 5 % Goat/Sheep serum diluted in PBTriton) for 2 to 3 hours. They were then incubated at room temperature overnight in polyclonal mouse serum primary antibody (Polyclonal IgG Rabbit Anti-GFP Primary Antibody, Invitrogen, A11122) diluted 1:500 in block solution. Embryos were washed in PBTriton once briefly and three times for one hour. They were incubated overnight 4 °C in Alexa Fluor 488 fluorescent anti-rabbit secondary antibody (Polyclonal IgG Alexa Fluor 488 donkey anti-rabbit, Invitrogen, A21206) diluted 1:200 in block solution. Embryos were then washed once briefly and three times for 30 minutes in PBTriton. They were stored in 50 % glycerol for imaging and storage.

Microscopy

Fish were mounted between bridged coverslips in methylcellulose for live embryos, anesthetized with 0.003 % MS222 (Sigma), and in 80 % glycerol for fixed embryos. Embryos were photographed using a Spot digital camera (supplier) mounted on an Eclipse E800 microscope (Nikon) or Axioplan 2 microscope (Zeiss) with DIC optics using a Spot digital camera mounted on a MZ12 microscope (Leica) with epi-illumination or Nikon sight DS-U1 camera (Nikon). To minimise the effects of the

developmental gradient along the body axis, melanocyte counts were performed on the head only, from the anteriormost region (forebrain) to the rear of the otic vesicle (posterior hindbrain); melanocytes were counted only in the region dorsal to the CNS (i.e the developing dorsal stripe).

Dendricity measurement

Dendricity was calculated as **R** *(R = P2/4pA, where A is the cell area and P the cell perimeter),* cell perimeter and area was measured using ImageJ software from images of cells taken using Eclipse E800 microscope (Nikon).

Ripley's K function analysis

To quantify and compare melanocyte organisation in DMSO treated embryos and BIO treated embryos the Multi-Distance Spatial Cluster Analysis, based on Ripley's K-Function, was performed using R statistical software (using packages "spatstat" and "dplyr" (R Core Team (2012)). Melanocyte positions were determined on the dorsal head of ten treated 72 hpf embryos for each conditions (DMSO and BIO treated) using comparable pictures. x and y coordinates for each melanocyte's position was determined using ImageJ. This data was then used to perform the Ripley's K function analysis which allows testing for random partition of the cells.

A Z-test allowed comparison of the two populations for cellular spatial organisation using the results of this analysis; the result was considered significant if $p<0.01$.

Statistics

Data were analysed by Prism 3.0 software GraphPadPrism 5.0 using unpaired t-test, α=0.05%, n=20 and fd= (x-2), with x = number of embryo tested.

Mathematical Modelling

Following the scheme of Supp. Fig. 3A and indicating the molecular species with their initials (except Tyrp1, indicated with T_y) we describe the behaviour of the GRN by the following set of ordinary differential equations:

$$\frac{dZ}{dt} = g_Z \frac{B}{K_B + B} - d_Z Z$$

$$\frac{dS}{dt} = g_S \left[\frac{\Phi_2 A(\Omega_1\Omega_2 + \Omega_1 H) + \Omega_2 M(\Phi_1\Phi_2 + \Phi_1 H) + \Omega_2 M\Phi_2 A}{(\Phi_1\Phi_2 + \Phi_2 A + \Phi_1 H)(\Omega_1\Omega_2 + \Omega_2 M + \Omega_1 H)} \right] - d_S S$$

$$\frac{dM}{dt} = g_M \left[\frac{(\Gamma_2 S + \Gamma_1 S^2)\widetilde{T}}{(\Gamma_{12} + \Gamma_2 S + \Gamma_1 S^2)(K_T + \widetilde{T})} \left(1 - \frac{\widetilde{M}T}{(K_T + T)(K_M + \widetilde{M})} \right) + \frac{\widetilde{M}\widetilde{T}}{(K_T + \widetilde{T})(K_M + \widetilde{M})} \right] - d_M M$$

$$\frac{dT}{dt} = g_T \frac{K_{WB} W_A(t) + K_{WA} W_B(t) + W_A(t) W_B(t)}{(K_{WB} + W_B(t))(K_{WA} + W_A(t))} - d_T T$$

$$\frac{dH}{dt} = g_H \frac{M}{K_{M1} + M} - d_H H$$

$$\frac{dT_y}{dt} = g_{Ty} \frac{M}{K_{M2} + M} - d_{Ty} T_y$$

$$\frac{dD}{dt} = g_D \frac{K_Z M + K_{M3} Z + MZ}{(K_Z + Z)(K_{M3} + M)} \frac{K_S}{K_S + S} - d_D D$$

$$\text{with : } \begin{cases} \widetilde{M} = M\Theta(M - \overline{M}) \\ \widetilde{T} = T\Theta(T - \overline{T}) \end{cases}, \quad \begin{cases} W_A(t) = W_A\left(\Theta(t - 30h) - \Theta(t - 15h)\right) G_{BIO} \\ W_B(t) = W_B \Theta(t - 30h) G_{BIO} \end{cases}$$

$$\text{and : } \Theta(x) = \begin{cases} 0 & x < 0 \\ 1 & x \geq 0 \end{cases}, \quad G_{BIO} = \begin{cases} 1 & \text{untreated} \\ (t - t^S_{BIO})\left(\Theta(t - t^E_{BIO}) - \Theta(t - t^S_{BIO})\right) & \text{BIO - treated} \end{cases}$$

All equations have been derived from the network scheme in Supp. Fig. 3A by applying the rules explained in Greenhill et al. (2011). In addition, here we consider β-catenin/Lef-1 (T) acting in conjunction with either Sox10 (S) or Mitfa (M) via an AND gate in order to activate the production of Mitfa itself. This means that Mitfa production is activated only when either of the two AND gates involving T (one with Sox10 and the other with Mitfa) is active. The AND gate with Sox10 is activated only when the concentration of T is larger than a given threshold $\overline{T}$. A second threshold $\overline{M}$ on the concentration of Mitfa is operative also on the self-activating loop of Mitfa.

The core of the network corresponds to what has already been modelled in Greenhill et al. (2011) with the addition of Wnt signaling. Wnt is assumed to have two components WntA (W_A in the equations above) and WntB (W_B) both activating transcription factor β-catenin/Lef-1 (indicated as T in the equations). The binding and unbinding dynamics of Wnt is assumed to be fast as compared to the other network reactions and therefore Wnt is assumed to be equilibrated at any time. The first component WntA is present only for a transient time between 15 and 30 hpf, while the second component WntB starts at 30 hpf and remains active throughout the whole differentiation process (see Supp. Fig. 3B). When these two components act together they guarantee specification and commitment of the melanocytes lineage. If only WntA is present then we have specification but no commitment (see Supp. Fig. 3C) while if only WntB is present no specification is observed (Supp. Fig. 3D). Notice that this mechanism relies on the presence of a threshold on the activation of the

AND gate between Sox10 and T which prevents the production of Mitfa and therefore the activation of Mitfa's feedback loop. In order to simulate the BIO-treatment we added a correction G_{BIO} to the W_A and W_B components, which amounts to a time-linear increase in Wnt when the BIO-treatment is applied between t^S_{BIO} and t^E_{BIO} (times of start and end of the treatment respectively) and is one when there is no BIO-treatment. Parameter values for the model are:

$$\begin{cases} g_Z = 0.1\,\text{nM/h} \\ g_S = 0.3\,\text{nM/h}, \\ g_M = 0.35\,\text{nM/h} \\ g_T = 1.3\,\text{nM/h} \\ g_H = 0.3\,\text{nM/h} \\ g_{Ty} = 3.1\,\text{nM/h} \\ g_D = 0.3\,\text{nM/h} \end{cases}, \quad \begin{cases} d_Z = 0.2\,\text{h}^{-1} \\ d_S = 0.3\,\text{h}^{-1} \\ d_M = 0.05\,\text{h}^{-1} \\ d_T = 0.6\,\text{h}^{-1} \\ d_H = 0.03\,\text{h}^{-1} \\ d_{Ty} = 0.6\,\text{h}^{-1} \\ d_D = 0.1\,\text{h}^{-1} \end{cases}, \quad \begin{cases} \Omega_1 = 1.92\,\text{nM} \\ \Omega_2 = 1.43\,\text{nM} \\ \Omega_{12} = 1.32\,\text{nM} \\ \Phi_1 = 2.0\,\text{nM} \\ \Phi_2 = 0.22\,\text{nM} \\ \Phi_{12} = 0.1\,\text{nM} \\ K_B = 0.175\,\text{nM} \\ K_{WA} = 0.5\,\text{nM}, \\ K_{WB} = 0.5\,\text{nM} \end{cases}, \quad \begin{cases} K_T = 7.8\,\text{nM} \\ K_M = 0.045\,\text{nM} \\ K_{M1} = 1.0\,\text{nM} \\ K_{M2} = 1.8\,\text{nM} \\ K_{M3} = 1.0\,\text{nM} \\ K_Z = 6.5\,\text{nM} \\ K_S = 1.2\,\text{nM} \end{cases}, \quad \begin{cases} W_A = 0.33\,\text{nM} \\ W_B = 0.25\,\text{nM} \\ \overline{M} = 0.01\,\text{nM}, \\ \overline{T} = 0.75\,\text{nM} \\ \Gamma_1 = 5.0\,(\text{nM}\cdot\text{h})^{-2} \\ \Gamma_2 = 4.5\,(\text{nM}\cdot\text{h})^{-2} \\ \Gamma_{12} = 1.8\,(\text{nM}\cdot\text{h})^{-2} \end{cases}$$

These values are chosen in accordance with measured values from the literature (Jin & Liao, 1999, Schwanhausser et al., 2011 and Eden et al., 2011 for Sox10, Jao et al., 2013 for Mitfa) and within similar ranges as in Greenhill et al. (2011) for those unknown. We have assumed the same affinity for the two Wnt components and larger concentration for W_A but the opposite assumption (different affinity and same concentration) would lead to the same results. A slower decay rate for Mitfa than the one used in Greenhill et al., 2011 produced a better quantitative agreement with BIO-treatment results.

Acknowledgements

We gratefully acknowledge M. Welham for provision of BIO stock for preliminary experiments in this study, S. Wilson for supplying the *Tg(top:GFP)* fish, N. Parkinson and Robert J. Burnside for technical advice, and H. Schwetlick and S. Mulnoz-Descalzo for helpful comments on the manuscript. Funding was provided by University of Bath Graduate Studentship (LV), and BBSRC grant BB/L00769X/1 (RNK) and BBSRC grant BB/L007789/1 (GA and AR), as well as NIH R01 DE013828 (TFS).

Alexander, C., Piloto, S., Le Pabic, P.,Schilling, TF. (2014), Wnt signalling interacts with bmp and edn1 to regulate dorso-ventral patterning and growth of the craniofacial skeleton. PLoS Genet, 7, e1004479

Aoude, AG.,Wadt, KA., Pritchard, AL., Hayward, N.K. (2015), Genetics of familial melanoma: 20 years after CDKN2A. Pigment Cell Melanoma Res, *28(2)*, 148-60.

Baddeley, A. and Turner,R . (2005). spatstat: An R Package for Analyzing Spatial Point Patterns. Journal of Statistical Software 12(6), 1-42.

Barker, N. (2008), The canonical Wnt/beta-catenin signaling pathway. Methods Mol Biol*, 468***,** 5-15.

Bellei, B., Flori, E., Izzo, E., Maresca, V. & Picardo, M. (2008), GSK3beta inhibition promotes melanogenesis in mouse B16 melanoma cells and normal human melanocytes. Cell Signal*, 20***,** 1750-61.

Bellei, B., Pitisci, A., Catricala, C., Larue, L. & Picardo, M. (2010), Wnt/beta-catenin signaling is stimulated by alpha-melanocyte-stimulating hormone in melanoma and melanocyte cells: implication in cell differentiation. Pigment Cell Melanoma Res*, 24***,** 309-25.

Carney, T. J., Dutton, K. A., Greenhill., E., Delfino-Machin, M., Dufourcq, P., Blader, P. & Kelsh, R. N. (2006), A direct role for Sox10 in specification of neural crest-derived sensory neurons. Development*, 133***,** 4619-30.

Cheli, Y., Ohanna, M., Balloti R. & Bertolotto, C. (2012), Fifteen-year quest for microphthalmia-associated transcription factor target genes. Pigment Cell Melanoma Res*, 23***,** 27-40.

Curran, K., Lister, J. A., Kunkel, G. R., Prendergast, A., Parichy, D. M. & Raible, D. W. (2010), Interplay between Foxd3 and Mitf regulates cell fate plasticity in the zebrafish neural crest. Dev Biol*, 344***,** 107-18.

Dorsky, R. I., Moon, R. T. & Raible, D. W. (1998), Control of neural crest cell fate by the Wnt signaling pathway. Nature*, 396***,** 370-3.

Dorsky, R. I., Moon, R. T. & Raible, D. W. (2000), Environmental signals and cell fate specification in premigratory neural crest. Bioessays*, 22***,** 708-16.

Dorsky, R. I., Sheldahl, L. C. & Moon, R. T. (2002), A transgenic Lef1/beta-catenin-dependent reporter is expressed in spatially restricted domains throughout zebrafish development. Dev Biol*, 241***,** 229-37.

Dunn, K. J., B. O. Williams, Y. Li and W. J. Pavan. (2000), Neural crest-directed gene transfer demonstrates Wnt1 role in melanocyte expansion and differentiation during mouse development. Proc Natl Acad Sci U S A **97**(18): 10050-10055.

Dutton, K. A., Pauliny, A., Lopes, S. S., Elworthy, S., Carney, T. J., Rauch, J., Geisler, R., Haffter, P. & Kelsh, R. N. (2001), Zebrafish colourless encodes sox10 and specifies non-ectomesenchymal neural crest fates. Development, *128*, 4113-25.

Eden, E., Geva-Zatorsky, N., Issaeva, I., Cohen, A., Dekel, E., Danon, T., Cohen, L., Mayo, A., Alon, U. (2011) Proteome half-life dynamics in living human cells. Science, *331*, 764-8.

Greenhill, E. R., Rocco, A., Vibert, L., Nikaido, M. & Kelsh, R. N. (2011), An iterative genetic and dynamical modelling approach identifies novel features of the gene regulatory network underlying melanocyte development. PLoS Genet, *7*, e1002265.

Hari, L., Miescher, I., Shakhova, O., Suter, U., Chin, L., Taketo, M., Richardson, W. D., Kessaris, N. & Sommer, L. (2012), Temporal control of neural crest lineage generation by Wnt/beta-catenin signaling. Development, *139*, 2107-17.

Herbarth, B., Pingault, V., Bondurand, N., Kuhlbrodt, K., Hermans-Bormeyer, I., Puliti, A., Lemort, N., Goossens, M., Wegner, M. (1998), Mutation of the Sry-related Sox10 gene in Dominant megacolon, a mouse model for human Hirschsprung disease. Proc Natl Acad Sci U S A, *95*, 5161-5.

Hodgkinson, C. A., Moore, K. J., Nakayama, A., Steingrimsson, E., Copeland, N. G., Jenkins, N. A. & Arnheiter, H. (1993), Mutations at the mouse microphthalmia locus are associated with defects in a gene encoding a novel basic-helix-loop-helix-zipper protein. Cell, *74*, 395-404.

Ikeya, M., Lee, S. M., Johnson, J. E., McMahon, A. P. & Takada, S. (1997), Wnt signaling required for expansion of neural crest and CNS progenitors. Nature, *389*, 966-70.

Jao, Le., Wente, SR., Chen, W. (2013) Efficient multiplex biallelic zebrafish genome editing using a CRISPR nuclease system. Proc Natl Acad Sci U S A,*110*, 13904-9.

Jin, E. J. & Thibaudeau, G. (1999), Effects of lithium on pigmentation in the embryonic zebrafish (Brachydanio rerio). Biochim Biophys Acta, *1449*, 93-9.

Jin, C & Liao, X. (1999), Backbone dynamics of a winged helix protein and its DNA complex at different temperatures: changes of internal motions in genesis upon binding to DNA. J Mol Bio *292*, 641-51.

Jonhson, S.L., Nguyen, A.N., Lister, J.A. (2011), mitfa is required at multiple stages of melanocyte differentiation but not to establish the melanocyte stem cell. Dev Biol. *350*, 405-413.

Kaufman, C.K., Mosimann, C., Fan, Z.P., Yang, S., Thomas, AJ., Ablain, J, Tan, J.L., Fogley, R.D., Van Rooijen, E., Hagedom, E.J., Ciarlo, C., White, R.M., Matos, D.A., Puller, A.C., Santeriello, C., Liao, EC., Young, R.A., Zon, L.I. (2016), A zebrafish melanoma model reveals emergence of neural crest identity during melanoma initiation. Science, *351,* 6272.

Kawasaki, A., Kumasaka, M., Satoh, A., Suzuki, M., Tamura, K., Goto, T., Asashima, M. & Yamamoto, H. (2008), Mitf contributes to melanosome distribution and melanophore dendricity. Pigment Cell Melanoma Res, *21*, 56-62.

Kelsh, R. N. (2006), Sorting out Sox10 functions in neural crest development. Bioessays, *28*, 788-98.

Kim, J. H., Sohn, K. C., Choi, T. Y., Kim, M. Y., Ando, H., Choi, S. J., Kim, S., Lee, Y. H., Lee, J. H., Kim, C. D. (2010), Beta-catenin regulates melanocyte dendricity through the modulation of PKCzeta and PKCdelta. Pigment Cell Melanoma Res, *23*, 385-93.

Kimmel, C. B., Ballard, W. W., Kimmel, S. R., Ullmann, B. & Schilling, T. F. (1995), Stages of embryonic development of the zebrafish. Dev Dyn, *203*, 253-310.

Korinek, V., Barker, N., Morin, P. J., Van Wichen, D., De Weger, R., Kinzler, K. W., Vogelstein, B. & Clevers, H. (1997), Constitutive transcriptional activation by a beta-catenin-Tcf complex in APC-/- colon carcinoma. Science, *275*, 1784-7.

Kumasaka, M., Sato, S., Yajima, I., Goding, C. R. & Yamamoto, H. (2005), Regulation of melanoblast and retinal pigment epithelium development by Xenopus laevis Mitf. Dev Dyn, *234*, 523-34.

Lee, H. Y., M. Kleber, L. Hari, V. Brault, U. Suter, M. M. Taketo, R. Kemler and L, Sommer. (2004), Instructive role of Wnt/beta-catenin in sensory fate specification in neural crest stem cells. Science, *303*, 1020-1023.

Lee, M., Goodall, J., Verastegui, C., Ballotti, R. & Goding, C. R. (2000), Direct regulation of the Microphthalmia promoter by Sox10 links Waardenburg-Shah syndrome (WS4)-associated hypopigmentation and deafness to WS2. J Biol Chem, *275*, 37978-83.

Levy, C., Khaled, M., Fisher, D.E. (2006), MITF: master regulator of melanocyte development and melanoma oncogene. Trends Mol Med., *12*, 406-14.

Lewis, J. L., Bonner, J., Modrell, M., Ragland, J. W., Moon, R. T., Dorsky, R. I. & Raible, D. W. (2004), Reiterated Wnt signaling during zebrafish neural crest development, Development, *131*, 1299-308.

Lister, J. A., Robertson, C. P., Lepage, T., Johnson, S. L. & Raible, D. W. (1999), nacre encodes a zebrafish microphthalmia-related protein that regulates neural-crest-derived pigment cell fate. Development, *126*, 3757-67.

Livak, K. J., Little, W. A., Stack, S. L. & Patterson, T. A. (1998), Polymorphisms in the human DNA ligase I gene (LIG1) including a complex GT repeat. Mutat Res, *406*, 1-8.

Martin, B.L, & Kimelman, D. (2012). Canonical Wnt signalling dynamically controls multiple stem cell decisions during vertebrate body formation. Dev. Cell 22, 223-232.

Moro, E., Ozhan-Kizil, G., Mongera, A., Beis, D., Wierzbicki, C., Young, RM., Bournele, D., Domenichini, A., Valdivia, L.E., Lum, L., Chen, C., Amatruda, J.F., Tiso N,Weidinger, G., Argenton, F. (2012), In vivo Wnt signaling tracing through a transgenic biosensor fish reveals novel activity domains. Developmental Biology, 366(2):327-40.

Mort, RL., Jackson, LJ., Patton, EE. (2015), The melanocyte lineage in development and disease. Development, *142*, 1387

Novak, A. & Dedhar, S. (1999), Signaling through beta-catenin and Lef/Tcf. Cell Mol Life Sci, *56*, 523-37.

Opdecamp, K., Nakayama, A., Nguyen, MT., Hodgkinson, C.A., Pavan, WJ, Arnheiter, H. (1997), Melanocyte development in vivo and in neural crest cell cultures: crucial dependence on the Mitf basic-helix-loop-helix-zipper transcription factor. Development, *124*, 2377-86.

Parichy, D. M., Ransom, D. G., Paw, B., Zon, L. I. & Johnson, S. L. (2000), An orthologue of the kit-related gene fms is required for development of neural crest-derived xanthophores and a subpopulation of adult melanocytes in the zebrafish, Danio rerio. Development*, 127***,** 3031-44.

Price, L. H. & Heninger, G. R. (1994), Lithium in the treatment of mood disorders. N Engl J Med*, 331***,** 591-8.

R Core Team (2012). R: A language and environment for statistical computing. R Foundation for Statistical Computing, Vienna, Austria. ISBN 3-900051-07-0

Ripley, B.D. (1977) Modelling spatial patterns (with discussion). *Journal of the Royal Statistical Society, Series B*, **39**, 172 – 212.

Schwanhäusser, B., Busse, D., Li, N., Dittmar, G., Schuchhardt, J., Wolf, J., Chen, W., Selbach, M. (2011), Global quantification of mammalian gene expression control, Nature *473*, 337-342.

Sineva, G. S. & Pospelov, V. A. (2010), Inhibition of GSK3beta enhances both adhesive and signaling activities of beta-catenin in mouse embryonic stem cells. Biol Cell*, 102***,** 549-60.

Speeckaert, R., Speeckaert, M.M., Van Geel, N. (2015), Why treatments do(n't) work in vitiligo: An autoinflammatory perspective. Autoimmun Rev, *14*, 332-40.

Steingrimsson, E., Copeland, N. G. & Jenkins, N. A. (2004), Melanocytes and the microphthalmia transcription factor network. Annu Rev Genet*, 38***,** 365-411.

Takeda, K., Yasumoto, K., Takada, R., Takada, S., Watanabe, K., Udono, T., Saito, H., Takahashi, K. & Shibahara, S. (2000), Induction of melanocyte-specific microphthalmia-associated transcription factor by Wnt-3a. J Biol Chem*, 275***,** 14013-6.

Thisse, C. & Thisse, B. (2008), High-resolution in situ hybridization to whole-mount zebrafish embryos. Nat Protoc*, 3***,** 59-69.

Tseng, A. S., Engel, F. B. & Keating, M. T. (2006), The GSK-3 inhibitor BIO promotes proliferation in mammalian cardiomyocytes. Chem Biol*, 13***,** 957-63.

Uong, A. & Zon, L. I. (2009), Melanocytes in development and cancer. J Cell Physiol*, 222***,** 38-41.

Van De Wetering, M., Cavallo, R., Dooijes, D., Van Beest, M., Van E.S, J., Loureiro, J., Ypma, A., Hursh, D., Jones, T., Bejsovec, A. (1997), Armadillo coactivates transcription driven by the product of the Drosophila segment polarity gene dTCF. Cell*, 88***,** 789-99.

Van Otterloo E., Li, W., Bonde, G., Day, K.M., Hsu, M-Y., Cornell, R.A. (2010), Differentiation of Zebrafish Melanophores Depends on Transcription Factors AP2 Alpha and AP2 Epsilon. PLoS Genet. *16*, e1001122.

Watanabe, K., Takeda, K., Yasumoto, K., Udono, T., Saito, H., Ikeda, K., Takasaka, T., Takahashi, K., Kobayashi, T., Tachibana, M. (2002), Identification of a distal enhancer for the melanocyte-specific promoter of the MITF gene. Pigment Cell Res*, 15***,** 201-11.

White, R.M., Cech, J., Ratanasirintrawoot, S., Lin, CY., Rahl, P.B., Burke, C.J., Langdon, E., Tomlinson, M.L., Mosher, J., Kaufman, C., Chen, F., Long, H.K., Kramer, M., Datta, S., Neuberg, D., Granter, S., Young, R.A., Morrison, S., Wheeler, G.N., Zon, LI. (2011), DHODH modulates transcriptional elongation in the neural crest and melanoma, Nature 471, 518-22.

Yamaguchi, Y. and V. J. Hearing. (2014). Melanocytes and their diseases. Cold Spring Harb Perspect Med 4(5).